Susana Isabel Pereira da Ponte

Licenciatura em Biologia

The role of Grainy head in epithelial tissue growth

Dissertação para obtenção do Grau de Mestre em
Genética Molecular e Biomedicina

Orientadora: Doutora Lara Carvalho, Investigadora, CEDOC/FCM-UNL

Júri:

Presidente: Doutor José Paulo Nunes de Sousa Sampaio
Arguente: Doutor Alisson Marques de Miranda Cabral Gontijo
Vogal: Doutora Lara Cristina de Jesus Carvalho

FACULDADE DE CIÊNCIAS E TECNOLOGIA
UNIVERSIDADE NOVA DE LISBOA

Setembro de 2014

Susana Isabel Pereira da Ponte

Licenciatura em Biologia

The role of Grainy head in epithelial tissue growth

Dissertação para obtenção do Grau de Mestre em
Genética Molecular e Biomedicina

Orientadora: Doutora Lara Carvalho, Investigadora, CEDOC/FCM-UNL

Júri:

Presidente: Doutor José Paulo Nunes de Sousa Sampaio
Arguente: Doutor Alisson Marques de Miranda Cabral Gontijo
Vogal: Doutora Lara Cristina de Jesus Carvalho

FACULDADE DE CIÊNCIAS E TECNOLOGIA
UNIVERSIDADE NOVA DE LISBOA

Setembro de 2014

The role of Grainy head in epithelial tissue growth

Part of the results of this thesis was presented in the following meetings:

Susana Ponte, Lara Carvalho, Inês Cristo and António Jacinto. *The role of Grainy head in epithelial tissue growth*. Drostuga 2013. Faro, Portugal, January 3rd 2014 [poster]

Susana Ponte, Lara Carvalho, Inês Cristo and António Jacinto. *The role of Grainy head in epithelial tissue growth*. Drostuga 2014. Tomar, Portugal, September 5th-6th 2014 [poster]

AGRADECIMENTOS

À minha orientadora, Lara Carvalho, pela paciência infinita, pelo apoio incondicional, pelas longas horas passadas a discutir o meu projeto, de volta do microscópio ou no friozinho da sala das moscas, e pelas noites mal dormidas a corrigir a tese.

Ao Prof. António Jacinto, pela oportunidade de trabalhar no seu laboratório e por acreditar nas minhas capacidades.

À Doutora Ana Madalena Ludovice, por ter sido o meu elo de ligação à FCT e se ter disponibilizado para me ajudar sempre que possível.

Ao “Tissue Morphogenesis and Repair Lab”, a minha família da Ciência, por todo o apoio durante esta fase da minha vida e por todos os belos momentos de convívio.

À Inês Cristo, a minha parceira do lado e a única pessoa que sabe (tão bem ou melhor do que eu) as maravilhas de estudar o Grh, por toda a ajuda neste projeto.

À minha família e amigos, que talvez nunca percebam porque é que eu estudo moscas, mas que ainda assim são os meus pilares.

ABSTRACT

The *grainy head* (*grh*) gene family encodes an important group of transcription factors that play a remarkably conserved role in epithelial organ development, epithelial barrier formation and epithelial repair upon damage in different organisms. The regulation and molecular targets of Grh are numerous and seem to highly depend on the studied developmental context and tissue.

Notably, the *grh* vertebrate homologs, called *grh-like* (*grhl*) genes, have recently been implicated in the pathogenesis of several human diseases, including tumor progression and metastasis in different types of cancer. However, the molecular mechanisms by which Grh exerts its function remain largely unknown.

The main goal of this project was to investigate the role of Grh in epithelial growth and maintenance using the *Drosophila melanogaster* (fruit-fly) wing as an *in vivo* model system. We wanted to understand how Grh influences cell proliferation and apoptosis, as well as cell polarity, cell adhesion and cytoskeleton.

Our results show that Grh is essential for epithelial cell survival, since both *grh* knockdown and overexpression lead to apoptosis. In addition, while *grh* knockdown induces an increase in cell proliferation, *grh* overexpression leads to the opposite phenotype, leading us to propose that this gene has a role in the control of cell proliferation. Grh seems to regulate both the expression and the localization of the cell adhesion protein E-cadherin in the wing disc epithelium. We also observed increased F-actin levels upon *grh* knockdown, suggesting that Grh can influence actin expression or dynamics.

In conclusion, our data suggest that Grh is a key transcription factor in the regulation of epithelial maintenance and integrity of the *Drosophila* wing imaginal disc.

Keywords: Grainy head; epithelia; growth; *Drosophila;* wing; wing imaginal disc

RESUMO

O gene "*grainy head*" (*grh*) pertence a uma família de fatores de transcrição, cuja função é importante no desenvolvimento de tecidos epiteliais, formação da barreira epitelial e sua reparação. Esta função é evolucionariamente conservada em diversos organismos, mas pouco se sabe sobre os mecanismos moleculares envolvidos. Grh regula numerosos genes e a sua ação parece depender do tecido e da fase de desenvolvimento.

Recentemente, os homólogos de *grh* presentes nos vertebrados, chamados genes "*grh-like*", têm sido implicados na patogénese de diversas doenças em humanos, em especial no desenvolvimento de tumores e metástases em diferentes tipos de cancro. Apesar de este gene ter sido alvo de vários estudos nos últimos anos, os mecanismos moleculares pelos quais atua são ainda em grande parte desconhecidos.

O principal objetivo deste trabalho foi então estudar o papel de Grh no crescimento e manutenção de tecidos epiteliais, nomeadamente na proliferação celular e apoptose, assim como na polaridade e adesão celulares e citoesqueleto. Para isso escolhemos usar a asa de *Drosophila melanogaster* (mosca-da-fruta) como modelo *in vivo*.

Os nossos resultados indicam que Grh é importante para a sobrevivência das células epiteliais pois a sua desregulação induz apoptose. Grh regula também a proliferação celular. Quando reduzimos a expressão de *grh* a proliferação celular aumenta, enquanto que a sobre-expressão de *grh* produz o efeito contrário. Para além dos efeitos na proliferação e apoptose, Grh parece também regular a expressão, assim como a localização celular, da molécula de E-caderina. Finalmente, detetámos ainda um aumento nos níveis de actina F quando reduzimos a expressão de *grh*, o que sugere que este gene poderá estar implicado na regulação do citoesqueleto de actina.

Em suma, os nossos resultados sugerem que Grh é um fator de transcrição essencial na regulação da manutenção e integridade epitelial do disco imaginal da asa de *Drosophila*.

Palavras-chave: Grainy head; crescimento; epitélios; *Drosophila*; asa; disco imaginal da asa

TABLE OF CONTENTS

INDEX OF FIGURES

INDEX OF TABLES

ABBREVIATIONS

µm – micrometer
A – anterior
AJ – adherens junction
Ap – apterous
BDSC - Bloomington *Drosophila* Stock Center
BMP - Bone Morphogenetic Protein
BSA - Bovine Serum Albumin
Casp3* - activated caspase-3
Celsr1 - Cadherin EGF LAG seven-pass G-type receptor 1
Cora – Coracle
D – Dorsal
DABCO - 1,4-Diazabicyclo[2.2.2]octane
DAPI - 4', 6-diamidino-2-phenylindole
Ddc - Dopa Decarboxylase
DGRC - *Drosophila* Genetics Resource Center
Diap1 - *Drosophila* inhibitor of apoptosis
Dpp – Decapentaplegic
Drice – *Drosophila* ICE/CED-3-related protéase
Dronc – *Drosophila* NEDD2-like caspase
DSHB - Developmental Studies Hybridoma Bank
dsRNA – double-stranded RNA
EGF - Epidermal Growth Factor
EMT - epithelial-to-mesenchymal transition
E-cad – E-cadherin
En – Engrailed
Ex – Expanded
Fas III - Fasciclin III
FLP - yeast recombinase flippase
FRT - Flippase Recognition Targets
GEF - Guanine Nucleotide Exchange factor
GFP – Green Fluorescent Protein
Grh – Grainy head
Grhl – Grainy head-like
h – hours
HCC - Hepatocellular Carcinoma
Hh - Hedgehog
Hid - Head Involution Defective
Hpo – Hippo

hpRNA – hairpin RNA
hs – heat-shock
IGF – Insulin Growth Factor
InR – Insulin Receptor
JNK - c-Jun NH(2)-terminal Kinase
L1 – first instar larva
L2 – second instar larva
L3 – third instar larva
MGR – Mammalian Grainy head
Mid-L3 – mid-third instar larva
min – minutes
miR – microRNAi
mm – millimeter
mRNA – messenger RNA
nls – nuclear localization signal/sequence
Nub – Nubbin
ON – overnight
P – posterior
PBS - Phosphate Buffer Saline
PCD – Programmed Cell Death
PCP – Planar Cell Polarity
PH3 – Phospho-Histone-H3
Ptc – Patched
PTEN - Phosphatase and Tensin homolog
PTK7 - Protein Tyrosine Kinase 7
Puc – Puckered
RhoA - Ras homolog gene family, member A
RISC - RNA-Induced Silencing Complex
RNAi- Ribonucleic Acid interference
Rpr – Reaper
RT – room temperature
SCC - Squamous Cell Carcinoma
Scrb1 - Scribble
Sinu – Sinuous
siRNA – small-interfering RNA
SJ – Septate Junction
SNP - Single Nucleotide Polymorphism
Stan - Starry night
Stit - Stitcher
TARGET - Temporal And Regional Gene Expression Targeting

TGase1 - Transglutaminase 1
TGF-beta - Transforming Growth Factor beta
TJ – Tight Junction
TOR - Target Of Rapamycin
ts – temperature sensitive
UAS – Upstream Activating Sequences
V – ventral
Vangl2 - Van Gogh-like 2
VDRC - Vienna *Drosophila* Resource Center
Wg – Wingless
Wnt – Wingless-related MMTV integration site
Wts – Warts
Yki – Yorkie

1. INTRODUCTION

1.1. *Drosophila* as model system

Drosophila melanogaster (hereafter called *Drosophila*), also known as fruit fly or vinegar fly, has been studied since the early 1900s. It is one of the most studied organisms in biological research, particularly in genetics and developmental biology. The fruit fly is easy and cheap to maintain, produces large numbers of offspring, and grows quickly. In addition, it has a well-defined mechanism of development, relatively simple and accessible anatomy and is amenable to powerful genetics and molecular biology techniques. Its complete genome was sequenced in 2000 and comparisons between the *Drosophila* and human genomes revealed that the fundamental biochemical pathways are fairly consistent (Adams *et al*., 2000). Moreover, approximately 75% of known human disease genes have homologs in the *Drosophila* genome, consolidating its importance as a model organism for medical research (Reiter *et al*., 2001).

1.1.1. *Drosophila* life cycle

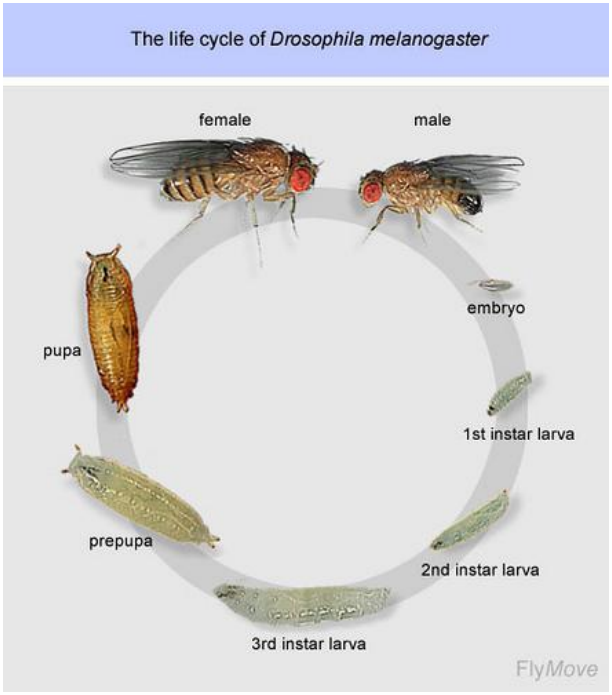

Figure 1.1. *Drosophila* life cycle. Adapted from Weigmann *et al*., 2013.

One of the many advantages of studying *Drosophila* is its short lifecycle (approximately 10 days at 25ºC). *Drosophila* is a holometabolous insect, meaning it undergoes a four-stage life cycle: egg, larva, pupa, and adult fly (Fig. 1.1). At 25°C, the embryo develops in the egg for 24 hours (h) before hatching as a larva. The larva eats and grows continuously in three different stages of development called instars. Larval stages are followed by pupariation, where the larva becomes an immotile pupa and metamorphosis takes place (Ashburner *et al*., 2005). During the metamorphosis stage, most of

the embryonic and larval tissues are destroyed. The adult tissues arise from groups of cells known as imaginal discs that have been set-aside since early embryonic development (Cohen, 1993).

1.1.2.Wing imaginal disc development

Cells in the imaginal discs proliferate extensively during the larval stages and, during metamorphosis, give rise to adult appendages, such as legs, wings, eyes and head cuticle, antennae and genitalia (Cohen, 1993) (Fig. 1.2, A).

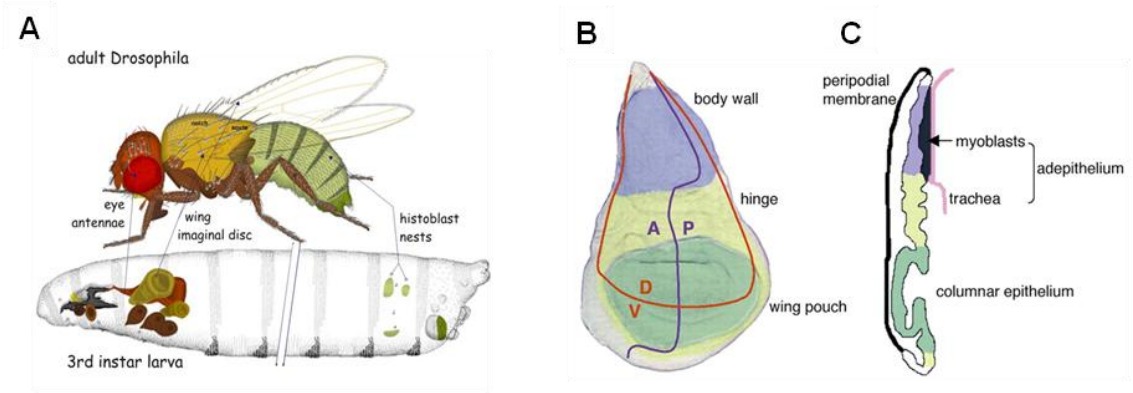

Figure 1.2. *Drosophila* imaginal discs. (A) The imaginal discs harbour cells that will give rise to the different body parts of the adult fly during metamorphosis. Adapted from St. Pierre *et al*., 2014. (B) Fate map of the wing disc showing the anterior-posterior (AP) and dorsal-ventral (DV) compartment boundaries and major regions in the disc: wing pouch (green), hinge (yellow) and body wall (blue). (C) Cell layers of the wing disc: peripodial membrane, columnar epithelium and adepithelium. B and C adapted from Butler *et al*, 2003.

The wing disc develops into the adult wing and the surrounding body wall tissue, the notum of the fly. It arises from a small group of 20–40 cells in the embryo (Lawrence and Morata, 1977) and proliferates extensively during larval development to achieve a final number of about 50000 cells (García-Bellido and Merriam, 1971). The wing disc is subdivided in different regions (Fig. 1.2, B), according to fate maps (Bryant, 1975): the wing pouch (green) gives rise to the wing blade, the hinge (yellow) constricts to form a link to the body wall (blue) of the fly. A longitudinal section shows that the wing disc is composed of three cell layers (Fig. 1.2, C): the columnar epithelium that differentiates into adult structures during metamorphosis (Fig. 1.3); the squamous epithelium, also called peripodial membrane, which has a leading role in disc eversion (Fig. 1.3, B) (Pastor-Pareja *et al*., 2004); and the adepithelium, composed of myoblasts, which develop into the flight muscles of the thorax and to tracheal cells of the larval and future adult airways.

The wing primordium is subdivided into groups of cells called compartments. Cells of adjacent compartments remain in contact during development of the wing disc but do not mix with each other (Lawrence and Morata, 1977). There are four compartments according to the main body axes: anterior (A), posterior (P), dorsal (D) and ventral (V) (Fig. 1.3, A).

Most of the research on growth in *Drosophila* uses the wing imaginal disc due to its structural simplicity and the abundance of genetic tools available. Isolated from most larval tissues, the wing disc constitutes a well-delimited developmental system. In addition, its development, patterning and growth

rate are very well known making it an ideal model system (James and Bryant, 1981; Bryant and Simpson, 1984; Madhavan and Schneiderman, 1977; Milán *et al*., 1996).

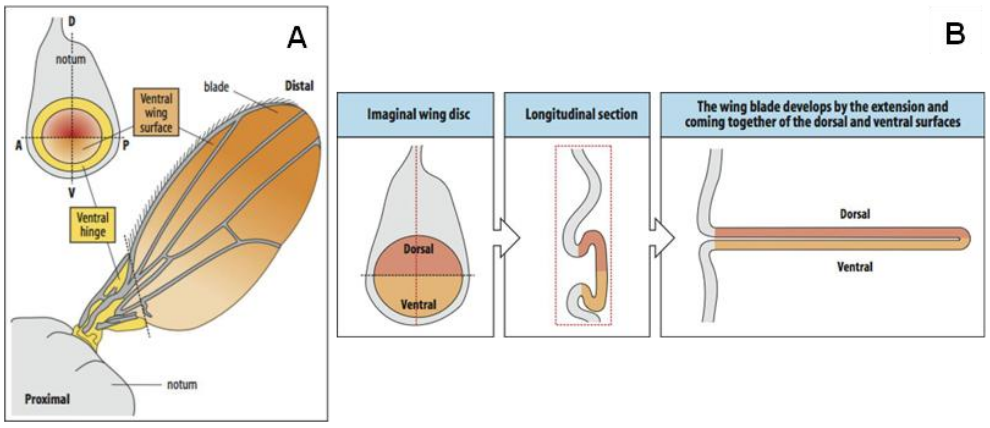

Figure 1.3. The wing imaginal disc gives rise to the adult wing and notum. (A) Schematic representation of the wing disc regions and boundaries (A: anterior; P: posterior; D: dorsal; V: ventral) and the corresponding regions in the adult wing. (B) Wing disc eversion. Adapted from Staveley, 2014.

1.1.3. Genetic tools

Over the past century, an incredible array of genetic tools has become available for *Drosophila* studies. Here we review some tools that have been used in this project:

1.1.3.1. Gal4/UAS system

The yeast transcriptional activator Gal4 is used to regulate gene expression in *Drosophila* by inserting the upstream activating sequence (UAS) to which it binds next to a gene of interest (gene X). To activate transcription, responder lines (UAS-GeneX) are mated to flies expressing Gal4 in a certain pattern, named the driver. The progeny will express gene X in a transcriptional pattern that reflects the Gal4 pattern of the respective driver thus allowing tissue-specific expression of the gene of interest (Fig. 1.4, A) (Brand and Perrimon, 1993). This system is widely used to modulate gene function by inducing the expression of RNAi against a specific gene and modified forms (e.g. dominant negative, constitutively active) of that gene (Elliot and Brand, 2008).

Over the years, this system has been refined to perform not only tissue/cell-type specific expression of certain genes, but also to allow temporal control. This technique relies on the expression of the yeast protein Gal80, which binds to Gal4 and prevents it from activating transcription (Lee and Luo, 1999; Suster *et al.*, 2004). Using the temporal and regional gene expression targeting (TARGET) technique (McGuire *et al*., 2003), in which a temperature sensitive version of Gal80 ($Gal80^{ts}$) (Matsumoto *et al.*, 1978) is expressed ubiquitously, we can control Gal4 repression just by transferring the flies to a different temperature. At 18ºC Gal80 is bound to Gal4, thus inhibiting Gal4-mediated transcription activation. When we shift the temperature to 29ºC, Gal4 is free and capable of activating transcription of our gene of interest (Fig. 1.4, B).

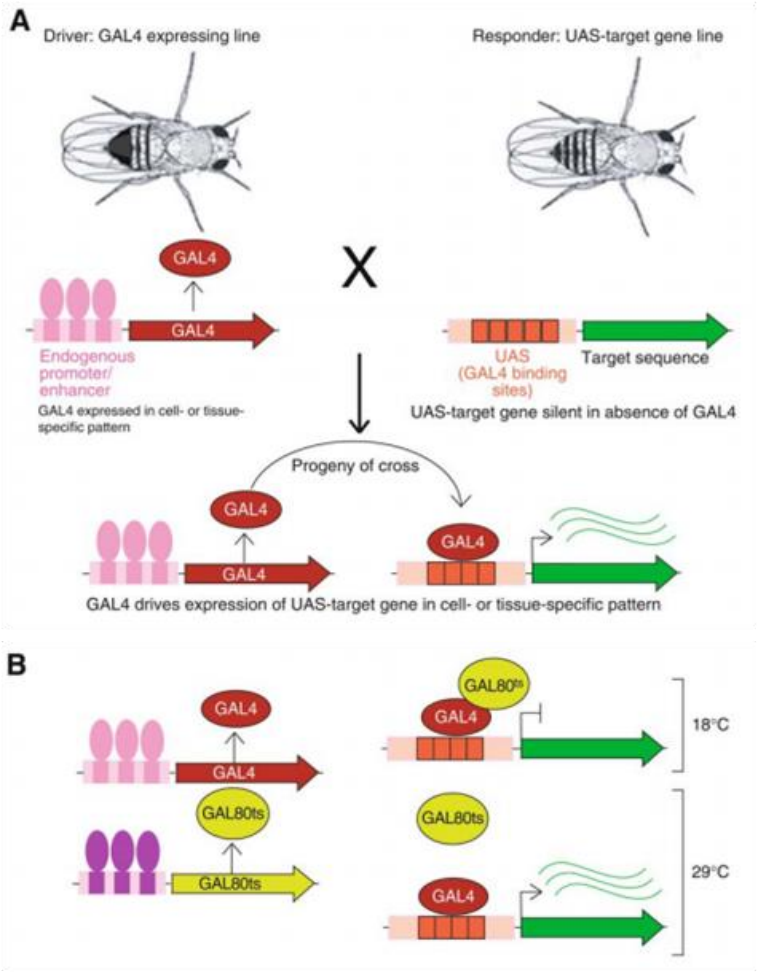

Figure 1.4. Schematic representation of the Gal4-based transgene expression. (A) Original scheme for the Gal4 system. (B) TARGET method of transgene regulation. Adapted from Elliot and Brand, 2008.

1.1.3.2. RNA interference

RNA interference (RNAi) is a widely used technique for gene silencing in organisms and cultured cells, and relies on sequence homology between double-stranded RNA (dsRNA) and target mRNA molecules (reviewed in Meister and Tuschl, 2004). This technique was first developed in *C. elegans* (Fire *et al*., 1998) but was quickly adapted to *Drosophila*, in which we can take advantage of the UAS/Gal4 system to express the dsRNA in a tissue specific and temporally controlled manner (Dietzl *et al*., 2007).

The RNAi construct contains an inverted repeat sequence, with homology to the target gene, so that it forms a hairpin structure upon transcription (Fig. 1.5). This structure is cleaved by the endogenous enzyme Dicer in small ~20bp fragments. These fragments serve as a template for the RNA-induced silencing complex (RISC) to specifically recognize and cleave the target mRNA, leading to its quick degradation (reviewed in Yamamoto-Hino and Goto, 2013).

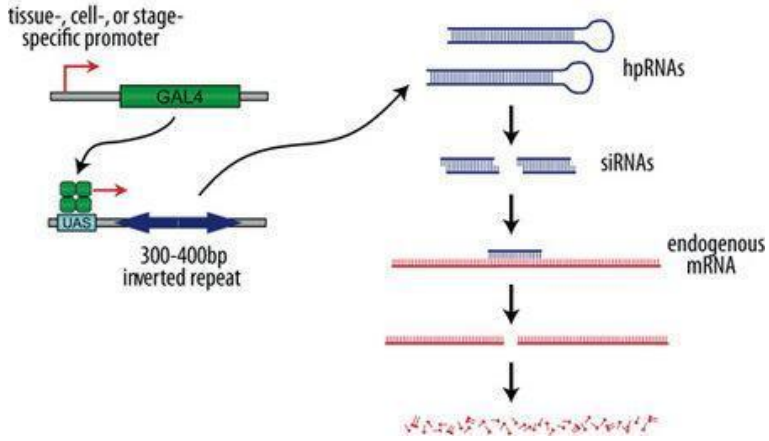

Figure 1.5. Transgenic RNAi in *Drosophila*. The Gal4/UAS system is used to drive the expression of a hairpin RNA (hpRNA). These RNAs are cleaved by Dicer into small interfering RNAs (siRNAs) which direct sequence-specific degradation of the target mRNA. Adapted from: Vienna *Drosophila* Resource Center (http://stockcenter.vdrc.at/control/howtornaidmel)

1.1.3.3. Clonal analysis

Genetic mosaic analysis is a powerful tool for understanding developmental and cell biology. Mosaic animals carry populations of cells with different genotypes. In *Drosophila*, this tool has been developed for many years and it is extremely useful to study genes that induce lethality when mutated in the entire organism. The induction of genetic mosaics thus allows the study of a population of mutant cells in a wild-type individual (Perrimon, 1998).

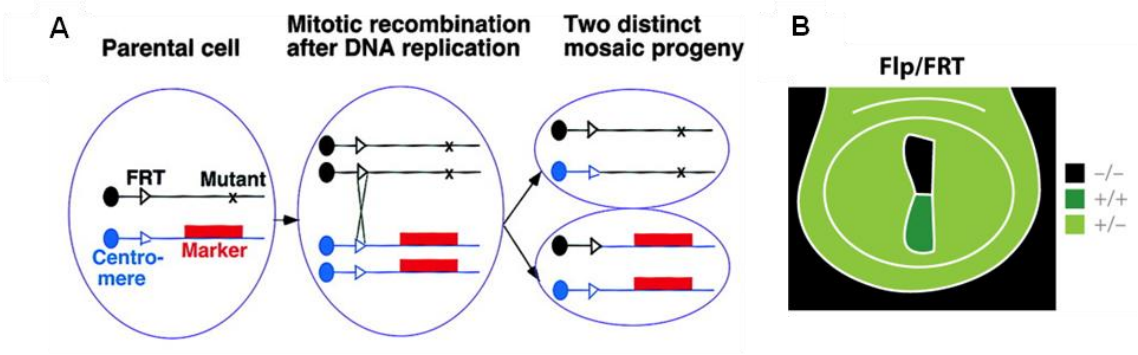

Figure 1.6. Mosaic analysis using the FLP/FRT technique. (A) Induction of somatic crossing-over between the two homologous chromosomes during mitosis. A heterozygous somatic cell (+/-) produces a homozygous mutant daughter cell (-/-) and a twin homozygous wild-type cell (+/+), resulting in a mosaic animal with three distinct genotypes (+/-, -/- and +/+). Adapted from Lee and Luo, 1999. (B) Schematic representation of mitotic recombination clones in the wing imaginal disc. Homozygous mutant clones are negatively labeled while the twin wild-type clone is distinguishable because it contains two copies of the marker. Adapted from Pastor-Pareja and Xu, 2013.

There are many ways of generating mosaics but here we will focus in the FLP/FRT technique. In this technique, the yeast recombinase flippase (FLP) is used to induce mitotic recombination and produce clones of homozygous mutant cells in a heterozygous animal. Expression of FLP in transgenic lines mediates the exchange of chromosome fragments between flippase recognition

targets (FRTs) inserted into fixed chromosomal locations (Golic and Lindquist, 1989). After chromosome segregation, one daughter cell is a homozygous mutant (-/-), thus becoming the founder of a mutant clone, whereas the other daughter cell is homozygous wild type (+/+), and will give rise to a twin clone (Figure 1.6, A). There are several ways to differentially label the mutant and wild type cells. For example, if a marker (e.g. green fluorescent protein, GFP) is placed distally to the FRT site, when mitotic recombination occurs the mutant clone will be marked by the absence of GFP while the twin clone will have two copies of GFP (Figure 1.6, B).

1.2. Growth control in *Drosophila*

From the large variation of sizes in the animal kingdom to the importance of growth control in many diseases, size control has long fascinated biologists. Tissue growth depends on three cellular processes: cell division, cellular growth and cell survival, each of them regulated by specific signaling pathways. These regulatory pathways control the cell cycle, protein synthesis and apoptosis and have to be coordinated to achieve proper tissue growth. Tissue growth is influenced by three types of inputs: factors from the animal's external environment (such as nutrients); hormones and neuronal signals that function systemically in the animal; and patterning cues arising within individual tissues (reviewed in Neto-Silva *et al.*, 2009).

We describe in more detail the regulation of growth by cell proliferation and apoptosis.

1.2.1. Cell proliferation

During most of the larval stages, cell division is actively induced in imaginal discs, leading to their growth (Garcia-Bellido and Merriam, 1971; Gonzalez-Gaitan *et al*., 1994). This stimulus is triggered by both extrinsic and intrinsic factors.

1.2.1.1. Extrinsic factors

Nutritional conditions regulate cell size and cell proliferation, and are thus essential for animal growth. The sensing and processing of nutrients is mediated by the conserved Insulin/IGF Receptor (InR) and TOR (Target Of Rapamycin) signaling pathways. In larval stages, when nutrients are abundant, circulating insulin levels increase and promote cell and tissue growth. Upon starvation, insulin levels are reduced and growth is arrested (reviewed in Grewal, 2008). Growth and body size are also influenced by physiological signals such as hormones and other systemic factors (reviewed in Edgar, 2006).

1.2.1.2. Intrinsic factors

Several studies show that imaginal disc growth does not only rely on extrinsic factors. Indeed, imaginal discs stop growing at the correct final size even when transplanted into the growth-permissive environment of an adult female fly abdomen (Bryant and Simpson, 1984). Although many growth regulators have been identified, the mechanisms are so not well understood. The overall

accepted view is that several evolutionarily conserved developmental signaling pathways - BMP/TGF-beta, Wnt, Hh, Notch, and EGF - are involved (reviewed in Neto-Silva *et al.*, 2009).

In addition, the recently discovered Hippo (Hpo) signaling pathway controls organ size in *Drosophila* and mammals by regulating cell growth, proliferation, and apoptosis in a coordinated manner (reviewed in Pan, 2007). The core of this pathway consists of two kinases, the Ste20-like kinase Hippo (Hpo) and the nuclear Dbf2-related (NDR) family kinase Warts (Wts), that when active suppress growth (Fig. 1.7). Hpo, facilitated by the scaffold protein Salvador (Sav), phosphorylates and activates Wts. Wts phosphorylates the transcriptional co-activator Yorkie (Yki), preventing its translocation from the cytoplasm to the nucleus. In contrast, when the pathway is inhibited, Yki is translocated to the nucleus and co-activates the expression of several target genes required for cell growth, survival and proliferation (reviewed in Zhao *et al*., 2010).

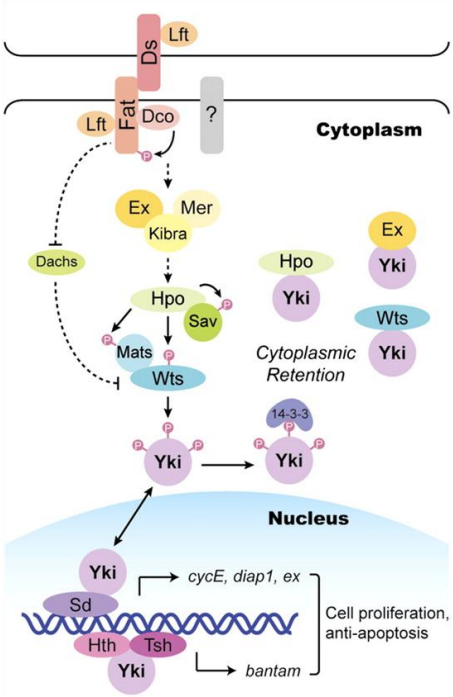

Figure 1.7. The Hippo pathway in *Drosophila*. Adapted from Zhao *et al*., 2010.

1.2.2. Apoptosis

Apoptosis is a form of programmed cell death (PCD) in which cells activate the machinery for their own destruction. Apoptotic cells undergo distinct morphological changes: the cell nucleus and cytoplasm condense and the cell is turned into fragments with preserved membranes that are rapidly eliminated by phagocytosis (Kerr *et al*., 1972).

Apoptosis is developmentally regulated and plays a crucial role in organogenesis and tissue remodeling. For example, apoptosis is necessary for the normal morphogenesis of the *Drosophila* larval head and of the adult leg joints (Lohmann *et al.*, 2002; Manjón *et al*., 2007). Additionally, apoptosis is critical to eliminate supernumerary, abnormal or malignant cells that may appear in development or during the life of an individual, not only in *Drosophila* but also in vertebrates (Igaki *et al*., 2009; Menéndez *et al*., 2010).

The molecular and subcellular events that characterize apoptosis are well known and are conserved among nematodes, insects and vertebrates. A critical step in apoptosis is the activation of caspases, a highly conserved family of cysteine proteases. These proteins are ubiquitously expressed and are synthesized as enzymatically inert zymogens, only becoming active upon specific death-inducing stimuli. The caspase family has been subdivided into two groups: initiator caspases (e.g. caspase-9) promote effector caspase activation; and effector caspases (e.g. caspase-3) execute apoptosis after being proteolytic processed by initiator caspases. Effector caspases degrade the cellular substrates resulting in cell death (reviewed in Hengartner, 2000).

In *Drosophila*, the NEDD2-like caspase (Dronc) acts as the primary initiator caspase, functionally similar to caspase-9 in mammals, whereas ICE/CED-3-related protease (Drice), functionally analogous to the mammalian caspase-3, functions as the main effector caspase (Kumar and Doumanis, 2000). The activity of caspases is subject to complex regulation. A key regulator of caspase activity is the *Drosophila* inhibitor of apoptosis (Diap1), which directly inhibits these apoptotic proteases thereby ensuring cell survival (Wilson *et al*, 2002). In turn, upon cell death inducing stimuli, Diap1 is inactivated by a group of factors encoded by the pro-apoptotic genes: *reaper* (*rpr*), *head involution defective* (*hid*), and *grim* (Goyal *et al*., 2000); thus allowing caspases to function (Fig. 1.8).

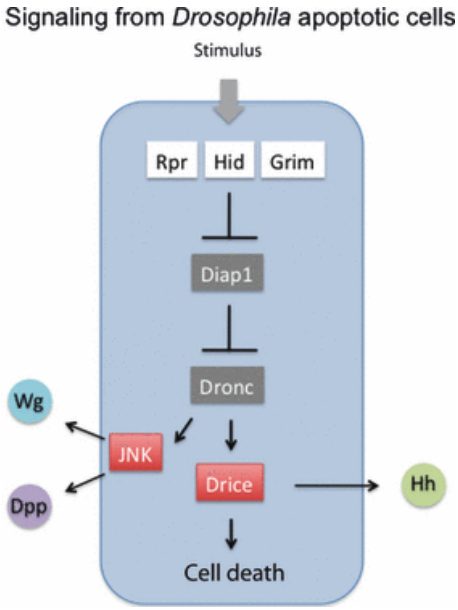

Figure 1.8. Signaling from *Drosophila* apoptotic cells. A stimulus leads to the activation of the pro-apoptotic genes *rpr*, *hid* and *grim* whose products bind to and inhibit Diap1. This allows Dronc to activate the effector caspase Drice, and importantly, the JNK pathway. JNK induces *dpp* and *wg*, which may promote proliferation in neighbor cells. The induction of the Hh signal is originated by a different mechanism, as it requires Drice activity. Also, unlike Dpp and Wg, it is emitted by non-proliferating cells. Adapted from Morata *et al.*, 2011.

Interestingly, apoptotic cells in *Drosophila* can ectopically activate the signaling genes *decapentaplegic* (*dpp*), *wingless* (*wg*) and *hedgehog* (*hh*) (Ryoo *et al*., 2004; Fan and Bergmann, 2008), which are known to play morphogenetic and growth control roles during development (reviewed in Tabata and Takei 2004). These observations have lead authors to suggest this activation as a mechanism of compensation for cell loss (Ryoo *et al*., 2004).

Another pathway implicated in stress-induced apoptosis both in *Drosophila* and in mammals is the c-Jun NH(2)-terminal kinase (JNK) pathway (reviewed in Dhanasekaran and Reddy, 2008). In *Drosophila*, this pathway plays a major role in inducing apoptosis upon irradiation: JNK signaling is massively activated and its knockdown significantly reduces apoptotic response in this situation (McEwen and Peifer, 2005). This could be due to the ability of JNK to induce the pro-apoptotic genes (McEwen and Peifer, 2005). Furthermore, JNK pathway is activated downstream of Dronc (Kondo *et al*., 2006) and appears to be involved in *dpp* and *wg* activation by apoptotic cells (Ryoo *et al*., 2004).

1.3. Grainy head and its roles in epithelia

The Grainy head (Grh) gene family encodes a group of transcription factors that contain an isoleucine-rich activation domain, a unique DNA-binding motif and a dimerization domain. They can dimerize and act as activators or repressors depending on the tissue and developmental context. Grh (also termed Elf-1 and NTF-1) was first discovered in *Drosophila* but it has homologs in nematodes, vertebrates and even Fungi. Whereas nematodes and *Drosophila* contain a single *grh* gene, vertebrates have multiple *grainy head-like* (*grhl*) homologues in their genomes. Mice and humans have three *grhl* genes (*grhl-1*, *grhl-2* and *grhl-3*) while zebrafish evolved four *grh* homologs (*grhl-1*, *grhl-2a*, *grhl-2b*, and *grhl-3*) (reviewed in Wang and Samakovlis, 2012).

In *Drosophila*, *grh* is expressed in the embryonic epidermis, the tracheal airways, the foregut and the hindgut (Bray and Kafatos, 1991; Hemphala *et al*., 2003), the embryonic central nervous system (CNS), the larval neuroblasts and optic lobes, and in imaginal discs (Uv *et al*., 1997). Although there is only one *grh* gene, alternative splicing generates a Grh-O isoform, exclusive of the neuroblasts in the CNS, and a Grh-N isoform, present in the other tissues (Uv *et al*., 1997).

The mouse *grhl* (*grhl1–3*) genes are expressed in the surface ectoderm and in other epithelial tissues, including the oral cavity, urogenital bladder, and gastrointestinal tract (Auden *et al*., 2006). Although there is extensive sequence identity among them, *grhl* genes have differential expression patterns and they are not fully redundant during development (Auden *et al*., 2006; Boglev *et al*., 2011).

1.3.1. Conserved roles of Grh

The Grh family of transcription factors has been shown to be crucial for the development and repair of epidermal barriers, from *Drosophila* to vertebrates (reviewed in Wang and Samakovlis, 2012). Here we describe some of the main conserved roles of Grh.

1.3.1.1. Epidermal barrier formation and repair

The name Grainy head comes from the phenotypes of *Drosophila* mutant embryos, which develop a granular head skeleton and a weak epidermal cuticle (Bray and Kafatos, 1991; Nüsslein-Volhard *et al*., 1984). The cuticle is a protective exoskeleton that isolates the animal body from the external environment. *grh* mutants have defects in cuticle formation that lead to their abnormal, flaccid appearance, in contrast to the wild type elongated hatched larva. There are also visible effects in

cuticle specializations: both the mouth hooks and the denticles of the hatched larva are poorly differentiated (Bray and Kafatos, 1991). Some of the Grh target genes responsible for cuticle formation, assembly, or hardening have been identified, such as *Ddc* (Bray and Kafatos, 1991). *Ddc* encodes the enzyme Dopa decarboxylase, involved in cross-linking proteins and lipids that strengthen the cuticle (Scholnick *et al.*, 1983). Additionally, Grh is crucial for the repair of the cuticle in wounded *Drosophila* embryos. Upon injury, Grh activates the expression of cuticle repair genes, such as *Ddc*, in cells surrounding epidermal wounds (Mace *et al*., 2005; Pearson *et al*., 2009). Besides cuticle repair, Grh is also required for the re-epithelization of the wounded epidermis by regulating the expression of the receptor tyrosine kinase Stitcher (Stit) (Wang *et al*, 2009).

In mice, the formation and maintenance of the epidermal barrier depends on Grhl-3. Mice lacking *grhl-3* show severe defects in skin barrier function, associated with impaired differentiation of the epidermis (Ting *et al*., 2005; Yu *et al*., 2006), due, in part, to diminished expression of a Grhl-3 target gene, *Transglutaminase 1* (*TGase1*), a protein/lipid cross-linking enzyme (Ting *et al*., 2005). Grhl-3 is also required for efficient wound healing (Ting *et al*., 2005).

1.3.1.2. Cell adhesion

In *Drosophila*, Grh seems to regulate components of the septate junctions (SJs), epithelial adhesive structures functionally analogous to vertebrate tight junctions (TJs). The SJ proteins Fasciclin III (FasIII), Coracle (Cora), and Sinuous (Sinu) contain Grh-binding sites in their regulatory regions. In addition, the protein levels of FasIII and Cora are reduced in *grh* mutant clones in the larva wing discs (Narasimha *et al*., 2008).

In mice, *grhl* genes regulate the expression of both TJ and adherens junction (AJ) components. While Grhl-2 was shown to regulate E-cadherin (AJs) and Claudin 4 (TJs) expression (Werth *et al*., 2010), Grhl-3 controls the TJ components Claudin 1 and Occludin in the epidermis (Yu *et al*., 2006).

1.3.1.3. Planar cell polarity

Other probable targets of Grh are components of the planar cell polarity (PCP) pathway. In *Drosophila*, Grh seems to directly regulate the transcription of the gene *starry night* (*stan*), a component of the PCP pathway. When *grh* mutant cells are induced in larval and pupal wing discs, Stan expression is greatly reduced and other planar polarity proteins fail to properly localize. These *grh* mutant cells eventually develop multiple and abnormal hairs (Lee and Adler, 2004).

In mice, Grhl-3 acts on the PCP pathway through the RhoA activator RhoGEF19 and interacts with the PCP genes *Vangl2*, *Celsr1*, *PTK7*, and *Scrb1* (Caddy *et al*., 2010).

1.3.2. Grh function in human disease

Given all the known roles of Grhl factors, it is not surprising that they are implicated in the pathogenesis of several human diseases. For example, a single nucleotide polymorphism (SNP) found in the *grhl-2* gene has been associated with age-related hearing loss (Peters *et al*., 2002; Van Laer *et al*., 2008). More recently, it has been reported that mutations in *grhl-2* lead to Autosomal-Recessive Ectodermal Dysplasia Syndrome (Petrof *et al*., 2014).

1.3.2.1. Grh and cancer in humans

Not only mutations, but also changes in *grhl* genes expression levels can promote disease, namely cancer. All three human Grhl factors have been implicated in different types of cancer.

Grhl-1, also known as Mammalian Grainy head (MGR)/LBP-32/TFCP2L2, acts as a tumor suppressor in neuroblastoma (Fabian *et al*., 2014).

Grhl-3 also behaves as a tumor suppressor in Squamous Cell Carcinoma (SCC) in mice (Bhandari *et al*., 2013) and humans (Darido *et al*., 2011). *grhl-3* expression is reduced in both mice and human skin SCCs and the deletion of the *grhl-3* gene leads to tumorigenesis in the skin of mice. Furthermore, two genes also associated with cancer, PTEN and the microRNA miR-21 have been identified as direct targets of Grhl-3 in skin carcinoma (Darido *et al*., 2011; Bhandari *et al*., 2013). Importantly, Grhl-3 was identified as one of the markers of the early stages of breast cancer (Panis *et al*., 2012; Xu *et al*., 2014).

Grhl-2 has been extensively associated with cancer. Grhl-2 functions as a tumor suppressor in gastric cancer. Previous work has shown that *grhl-2* expression is significantly downregulated in gastric cancer and overexpression of *grhl-2* is sufficient to inhibit proliferation and promote apoptosis (Xiang *et al*., 2013). Recent studies have also revealed a role of Grhl-2 in breast cancer. Knockdown of *grhl-2* expression in a human mammary epithelial cell line leads to typical epithelial-to-mesenchymal transition (EMT) features, such as downregulation of E-cadherin and upregulation of the transcription factor Snail (Xiang *et al*., 2012). Other authors further confirmed that Grhl-2 expression suppresses EMT using other cell lines (Cieply *et al*., 2012, 2013). Although these studies suggest that *grhl-2* is a tumor suppressor gene, other observations have revealed that it can also act as an oncogene. Two independent studies have shown that overexpression of *grhl-2* in breast cancer cell lines induces changes in cell morphology and increase proliferation leading to tumor growth and metastasis (Werner *et al*., 2013; Xiang *et al*., 2012). Additionally, downregulation of Grhl-2 expression inhibits the growth of hepatoma cells and gain of Grhl-2 might be a predictive marker for Hepatocellular Carcinoma (HCC) recurrence (Tanaka *et al*. 2008).

To summarize, in the past years, the expression of *grhl* genes has been characterized in different types of cancer and several Grhl targets have been identified, revealing a clear connection between Grhl factors and cancer. Nevertheless, the molecular mechanisms by Grhl proteins exert their function are not yet fully understood and some studies show contradictory results. Therefore, more research is needed to enlighten the function of this family of transcription factors in cancer development.

1.4. Objectives of this thesis

The Grh gene family encodes an important group of transcription factors that regulate the development and repair of epidermal tissues from nematodes and insects to vertebrates. Recently, Grhl factors have been implicated in the pathogenesis of several human diseases, including tumor progression and metastasis in different types of cancer. However, the molecular mechanisms by which these genes exert their functions remain largely unknown. In order to decipher the roles of these genes in an *in vivo* context we chose *Drosophila* as a model system. The simplicity and genetic amenability of this organism, together with fact that *Drosophila* contains only one *grh* gene in its genome, make it an ideal system to study this gene family.

The main goal of this project was thus to further understand the function of Grh in epithelial growth control and homeostasis. For that we took advantage of the *Drosophila* wing imaginal disc as a model system. Our objectives were the following:

I. To investigate the role of Grh in cell proliferation and apoptosis, two basic cellular processes involved in the control of growth.

II. To study the influence of Grh in cell polarity, cell adhesion and cytoskeleton.

2. . MATERIALS AND METHODS

2.1. *Drosophila* stocks and husbandry

Drosophila stocks used in this project are described in Table 2.1. Flies were kept at 25ºC in vials containing fly food (a mixture of water, agar, sugar, corn meal, yeast, and fungicides) supplemented with dry yeast to stimulate egg laying. Males and female virgins were collected and kept at 18ºC until crosses were performed.

Table 2.1. Detailed list of *Drosophila* stocks used in this project. BDSC: Bloomington *Drosophila* Stock Center; VDRC: Vienna *Drosophila* Resource Center; Kyoto DGRC: Kyoto *Drosophila* Genetics Resource Center.

Name	Genotype/Construct	From
w^{1118}	w[1118]	BDSC #3605
UAS-*grh*	P{UAS-*grh*.K}	Kim and McGinnis, 2010
grh RNAi	P{KK109135}VIE-260B	VDRC #101428
*tub*P-Gal80^{ts}	w*; snaSco/CyO; P{tubP-Gal80^{ts}}7	BDSC #7018
*tub*P-Gal80^{ts}	w*; P{tubP-Gal80^{ts}}20; TM2/TM6B, Tb1	BDSC #7019
MS1096-Gal4	w1118 P{GawB}Bx^{MS1096}	BDSC #8860
hh-Gal4	hh-Gal4, UAS-GFP/TM6b	T. Tabata
en-Gal4	w; en-Gal4, UAS-GFP/CyO	BDSC #6356
nub-Gal4	w; nub-Gal4, UAS-GFP	Calleja *et al*., 1996
ptc-Gal4	w*; P{GawB}ptc$^{559.1}$	BDSC #2017
ap-Gal4	y[1] w[1118]; P{w[+mW.hs]=GawB}ap[md544]/CyO	BDSC #3041
ex-LacZ	w; ap-Gal4, ex^{697}/ CyO	Hamaratoglu *et al*., 2006
puc^{E69}	w*; cno3 P{A92}pucE69 / TM6B,abdA-*LacZ*	Kyoto DGRC #109029
FRT42D-*grh*	y[d2] w[1118] P{ry[+t7.2]=ey-FLP.N}2 P{GMR-*lacZ*.C(38.1)}TPN1; P{ry[+t7.2]=neoFRT}42D P{w[+mC]=lacW}*grh*[s2140] /CyO y[+]	Kyoto DGRC #111112
FRT42D-ubiGFPnls	w1118; P{neoFRT}42D P{Ubi-GFP(S65T)nls}2R/CyO	BDSC #5626
hs-FLP	yw, hsflp; Sco/CyO	BDSC #1929

To modulate *grh* expression, we either expressed *grh* RNAi to knockdown *grh*, or expressed UAS-*grh* to overexpress this gene, and observed their phenotypes in wing disc/adult wing growth and development. The UAS-*grh* flies were kindly supplied by W. McGinnis. The construct consists of a full-length copy of the *grh* gene preceded by UAS sequences (Kim and McGinnis, 2010). The *grh* RNAi flies were obtained from Vienna *Drosophila* Resource Center (VDRC). The RNAi construct contains UAS sequences fused to an inverted repeat sequence with homology to the *grh* gene. We crossed w^{1118} flies with Gal4-driver flies and used the progeny as controls.

We expressed *grh* (UAS-*grh*) or RNAi for *grh* in different parts of the wing disc, using different

drivers. We also expressed UAS-GFP to visualize the regions where the constructs were expressed. The Gal4 drivers used in this project were: *patched*-Gal4 (*ptc*-Gal4), *engrailed*-Gal4 (*en*-Gal4), *hedgehog*-Gal4 (*hh*-Gal4), *apterous*-Gal4 (*ap*-Gal4), *nubbin*-Gal4 (*nub*-Gal4) and *MS1096*-Gal4. The expression patterns are described in Flybase (http://flybase.org/, St. Pierre *et al*., 2014). With the exception of the *MS1096*-Gal4 and *nub*-Gal4 drivers, which are described as wing disc restricted, the other drivers are also expressed in other organs of the fly in different developmental stages. In the wing imaginal disc, *hh*-Gal4 and *en*-Gal4 drive gene expression in the posterior compartment, *ap*-Gal4 in the dorsal compartment, *ptc*-Gal4 in the anterior-posterior boundary, *nub*-Gal4 in the wing pouch, and *MS1096*-Gal4 in the dorsal part of the wing pouch. *hh*-Gal4, *nub*-Gal4, and *ex-lacZ* reporter were kindly supplied by F. Janody.

2.2. Experimental assay

To test the different Gal4 drivers, we crossed female virgins expressing UAS-*grh* or *grh* RNAi with males expressing Gal4 drivers and raised them at 25ºC.

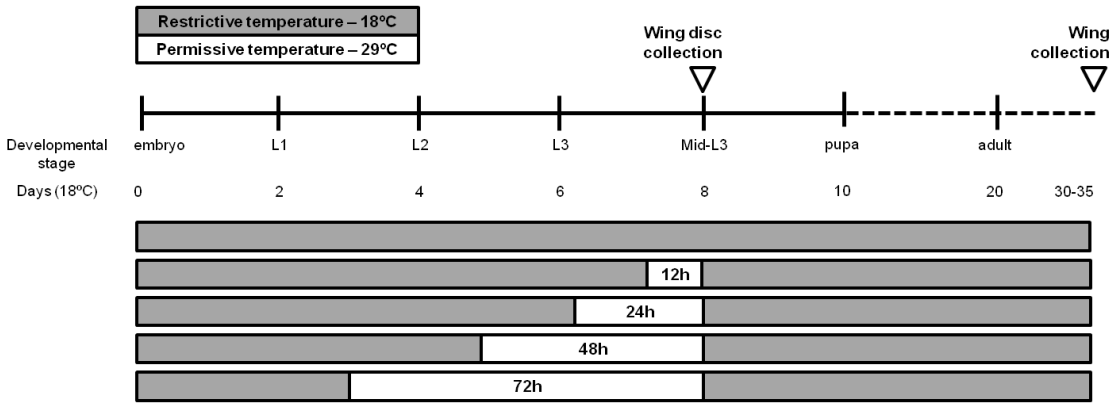

Figure 2.1. Temporal control of *grh* expression. After 3, 5, 6 or 7.5 days at 18ºC, the larvae were incubated at Gal4 permissive temperature (29ºC) for different periods of time (0h, 12h, 24h, 48h and 72h, respectively) to achieve different levels of *grh* knockdown and overexpression. After *grh* expression manipulation, the larvae were transferred to 18ºC to complete fly development. L1: first instar larva; L2: second instar larva; L3: third instar larva; Mid-L3: mid-third instar larva. *Drosophila* development duration is represented in days, according to fly development at 18ºC (2 days between each developmental stage; after pupal stage, the dashed line indicates a different timescale).

To perform temporal control of gene expression, we took advantage of the TARGET technique in which Gal4 expression is inhibited by Gal80^{ts} at restrictive temperatures (18ºC) but active at permissive temperatures (29ºC) (see INTRODUCTION) (McGuire *et al*., 2003). Our experimental design is shown in Figure 2.1. Eggs were collected for 6-12 h and embryos and early larvae were kept at Gal4 restrictive temperature (18ºC) to inhibit gene expression. To activate the expression of our genes/constructs of interest (UAS-*grh* and *grh* RNAi), larvae were transferred to 29ºC. Different periods of time (12, 24, 48 and 72 h) were tested to determine the best conditions to obtain a wing disc or wing phenotype without affecting fly survival. After 3, 5, 6 or 7.5 days, the larvae were incubated at 29ºC for 72, 48, 24 or 12 h, respectively. Mid-third instar (Mid-L3, wandering stage) larvae were collected to perform immunostainings and the remaining larvae were transferred to 18ºC

to allow them to reach adult stage. To analyse the wing phenotype, adult flies (approximately 10-15 days old) were collected and stored at -20ºC until wing mounting was performed.

2.3. Generation of *grh* mutant clones

To generate *grh* mutant clones marked by the absence of GFP in the wing disc, *y*,*w*; FRT42D-*grh*/CyO males were crossed to *y*,*w*,hsFLP; FRT42D-ubiGFPnls/CyO females. Mitotic recombination between homologous chromosomes generates homozygous *grh* mutant cells, with loss of the GFP marker. We used a heat-shock inducible flippase (hsFLP) to induce mitotic recombination, so the progeny was heat-shocked for 1 h at 37°C at 24 h of larva development, after a 24 h egg collection. All experiments were performed at 25°C. GFP-positive mid-L3 larvae were dissected 72 h after heat-shock. Dissection and immunostaining protocols are described below.

2.4. Immunochemistry

2.4.1. Larvae dissection

Mid-L3 larvae were dissected in ice-cold Phosphate Buffer Saline (PBS), using forceps (Student Dumont #5 Forceps, Fine Science Tools) as described by Purves and Brachmann, 2007. While holding the anterior part of the larva, the posterior part was removed by pulling it with a forcep. After that, one forcep was inserted in the larval mouth and the other was used to turn the larva inside out, exposing the internal organs. Most of the internal larval contents (e.g. fat body and gut) were removed and the remaining tissue, containing the imaginal discs still attached to the larval head, was transferred to a 1,5mL microtube with ice-cold PBS1x, and was kept on ice until fixation. No more than 10 larvae were added to each microtube, to prevent inefficient staining.

2.4.2. Immunofluorescence protocol

Dissected larvae were fixed for 20 minutes (min) in 4% Formaldehyde (Sigma-Aldrich) in PBS1x at room temperature (RT) and washed 4x10 min with PBST [PBS 1X + 0,1% Triton-X, (Acros Organics)]. Larvae were incubated in blocking solution [0,5% Bovine Serum Albumin (BSA, Sigma-Aldrich) in PBST] for 45 min, followed by an overnight (ON) incubation at 4ºC with primary antibodies (Table 2.2) diluted in blocking solution. Larvae were rinsed 4x10 min with blocking solution and incubated with secondary antibodies (Table 2.3) for 2 h at RT.

Phalloidin staining was performed to label actin. Alexa Fluor® 568 Phalloidin (Life Technologies) (1:100 dilution) was added to the secondary antibody incubation. DAPI solution (4', 6-diamidino-2-phenylindole, Sigma-Aldrich, 1: 500 in PBST) was added in the last 15 min of secondary antibody incubation.

Larvae were rinsed 5x10 min with PBST before adding anti-fading mounting media [2% DABCO (1,4-Diazabicyclo[2.2.2]octane, Sigma-Aldrich) + PBS 1x (1:4) + glycerol]. Stained larvae were kept at 4ºC until mounting.

Table 2.2 Detailed description of the primary antibodies. DSHB: Developmental Studies Hybridoma Bank.

Antigen	Supplier	Reference	Host	Working dilution
Grainy head	Kindly provided by C. Samakovlis		rabbit	1:1000
Cleaved Caspase-3 (Asp175)	Cell Signaling Technology (CST)	#9661	rabbit	1:50
Phospho-Histone H3 (Ser10)	Millipore	06-570	rabbit	1:50
GFP (clones 7.1 and 13.1)	Roche	11814460001	mouse	1:500
GFP	Life Technologies	A-11122	rabbit	1:2000
DE-cadherin	DSHB	DCAD2	rat	1:30
Wingless	DSHB	4D4	mouse	1:10
β-Galactosidase	Life Technologies	A-11132	rabbit	1:2500
Crumbs	DSHB	Cq4	mouse	1:3

Table 2.3 Detailed description of the secondary antibodies.

Antibody	Reference	Supplier	Working dilution
Alexa Fluor 488 goat anti-mouse IgG	A-11001	Life Technologies	1:250
Alexa Fluor 488 anti-rabbit IgG (H+L)	A-11008		
Alexa Fluor® 488 Goat Anti-Mouse IgG1 (γ1)	A-21121		
Alexa Fluor® 488 Donkey Anti-Rat IgG (H+L)	A-21208		
Alexa Fluor® 568 goat anti-rabbit IgG	A-11036		
Cy5® Goat Anti-Rat IgG (H+L)	A-10525		

2.4.3. Wing disc dissection and mounting

Stained wing discs were detached from the remaining larval tissues using forceps (Student Dumont #5 Forceps, Fine Science Tools) and mounted in a drop of mounting media [2% DABCO (1,4-Diazabicyclo[2.2.2]octane, Sigma-Aldrich)] between two 24x60 millimeter (mm) coverslips. The coverslips were separated by one-coverslip-high bridge to prevent tissue damage, and sealed using nail polish.

2.5. Wing mounting

Wings were removed from adult flies immersed in 100% ethanol using forceps (Student Dumont #5 Forceps, Fine Science Tools). Dissected wings were transferred to a microscope slide and ethanol allowed to evaporate. A drop of Euparal medium (Fisher Scientific) was added and a glass coverslip placed on top. Preparations were flattened at 65ºC ON with a weight (~2g) on top. Slides were stored at RT.

2.6. Imaging

Wing disc imaging was performed on a LSM 710 (Carl Zeiss) confocal microscope using a 40X water objective. Adult flies images were obtained using the SteREO Discovery.V12 stereomicroscope (Carl Zeiss). Wing images were taken using a SteREO Discovery.V8 (Carl Zeiss) stereomicroscope.

2.7. Image analysis

Images were analysed using Fiji (Image J, NIH). Figures were made using Adobe Photoshop and Adobe Illustrator.

Wing size was determined by measuring posterior and anterior compartment areas. We compared wings from the same gender (males) of each genotype. At least eight wings per condition were analyzed.

Proliferation was quantified by counting the number of phospho-histone-H3 positive cells in the wing pouch region. We also quantified the wing pouch posterior and anterior area, to normalize the number of cells per area. At least six wing discs per condition were analysed.

Calculations were made using Excel (Microsoft) and Prism (GraphPad) was used to make graphs and perform statistical analysis. Statistical significance was determined by comparison to controls, using a two-tailed unpaired Student’s t-test.

3. RESULTS

3.1. Impact of *grh* expression manipulation in fly development and survival

To evaluate the impact of *grh* knockdown and overexpression in wing growth and development, we expressed *grh* RNAi (knockdown) and *grh* full-length (overexpression) in a tissue-restricted manner by using different Gal4-drivers. We tested *MS1096*-, *nub*-, *ap*-, *hh*-, *ptc*- and *en*-Gal4, which are all expressed during wing development, but in different domains and levels in the wing disc. At 25ºC, which is the optimal temperature for fly development, both knockdown and overexpression of *grh* lead to 100% lethality before pupal stages, except in the case of *MS1096*-Gal4 (where it was possible to collect adult flies) (Fig. 3.1). When expressing *grh* RNAi under the control of *MS1096*-Gal4 (Fig. 3.1, B), adult flies presented necrotic and small wings in contrast to controls (Fig. 3.1, A). In some cases, the wings also showed blisters. When we overexpressed *grh* (Fig. 3.1, C) only a few flies ecloded, with very small and deficient wings.

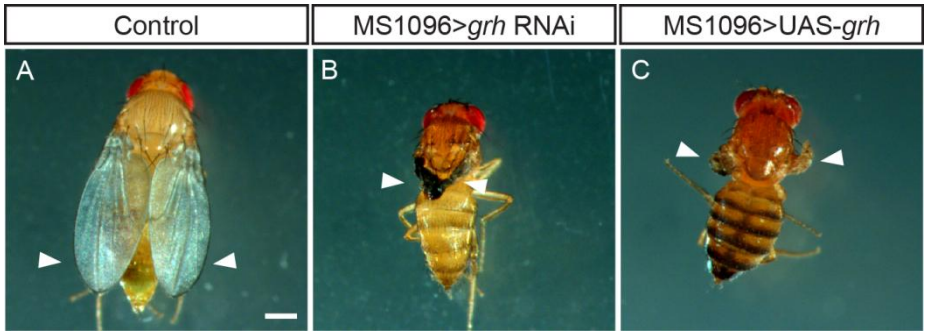

Figure 3.1. Manipulation of *grh* expression levels specifically in the wing imaginal disc leads to defects in the *Drosophila* adult wing. (A), adult wing phenotype of control (*MS1096*-Gal4/w^{1118}), (B), *grh* knockdown (*MS1096*-Gal4/+;*grh*RNAi/+), and (C), *grh* overexpressing (*MS1096*-Gal4/+;;UAS-*grh*/+) flies. Arrowheads point to the wings. Scale bar=500 µm.

Because the effects of manipulating *grh* expression were so dramatic, even using tissue-specific drivers, we decided to perform temporal control of *grh* expression. From all the drivers we tested, we chose the *hh*-Gal4 driver to perform the majority of the experiments described in this thesis. Although its expression is not restricted to the wing disc, this driver has the advantage of being expressed only in the posterior compartment of the wing disc, thus allowing us to use the anterior compartment as an internal control. Using this strategy we could assess whether the observed phenotypes were cell autonomous or non-cell-autonomous.

To perform temporal control of *grh* expression, we kept the flies at Gal4 restrictive temperature (18ºC) for most of its development. To activate the expression of UAS-*grh* and *grh* RNAi, larvae were typically transferred to 29ºC for 12 h, 24 h, 48 h and 72 h; in some cases not all these conditions were tested due to time or technical constraints.

From 48 h of knockdown onwards, we observed increasing levels of lethality during late pupal stages. Overexpression of *grh* induced more severe effects on fly development and survival. Flies developed until adulthood when we overexpressed *grh* for 12 h but longer periods of UAS-*grh*

expression led to increasing levels of lethality at larval or early pupal stages. We also observed a developmental delay in the surviving embryos and larvae.

Since the severity of the defects caused by *grh* knockdown and overexpression were different, we determined the optimal conditions to study their effects on wing development. Regarding *grh* overexpression, 12 h of UAS-*grh* expression seemed to be ideal as it was sufficient to induce a phenotype without causing lethality. In the case of *grh* RNAi, we expressed it for 72 h for a strong knockdown but also looked at intermediate levels of knockdown to understand the phenotype progression.

3.2. *grh* expression in the wing imaginal disc

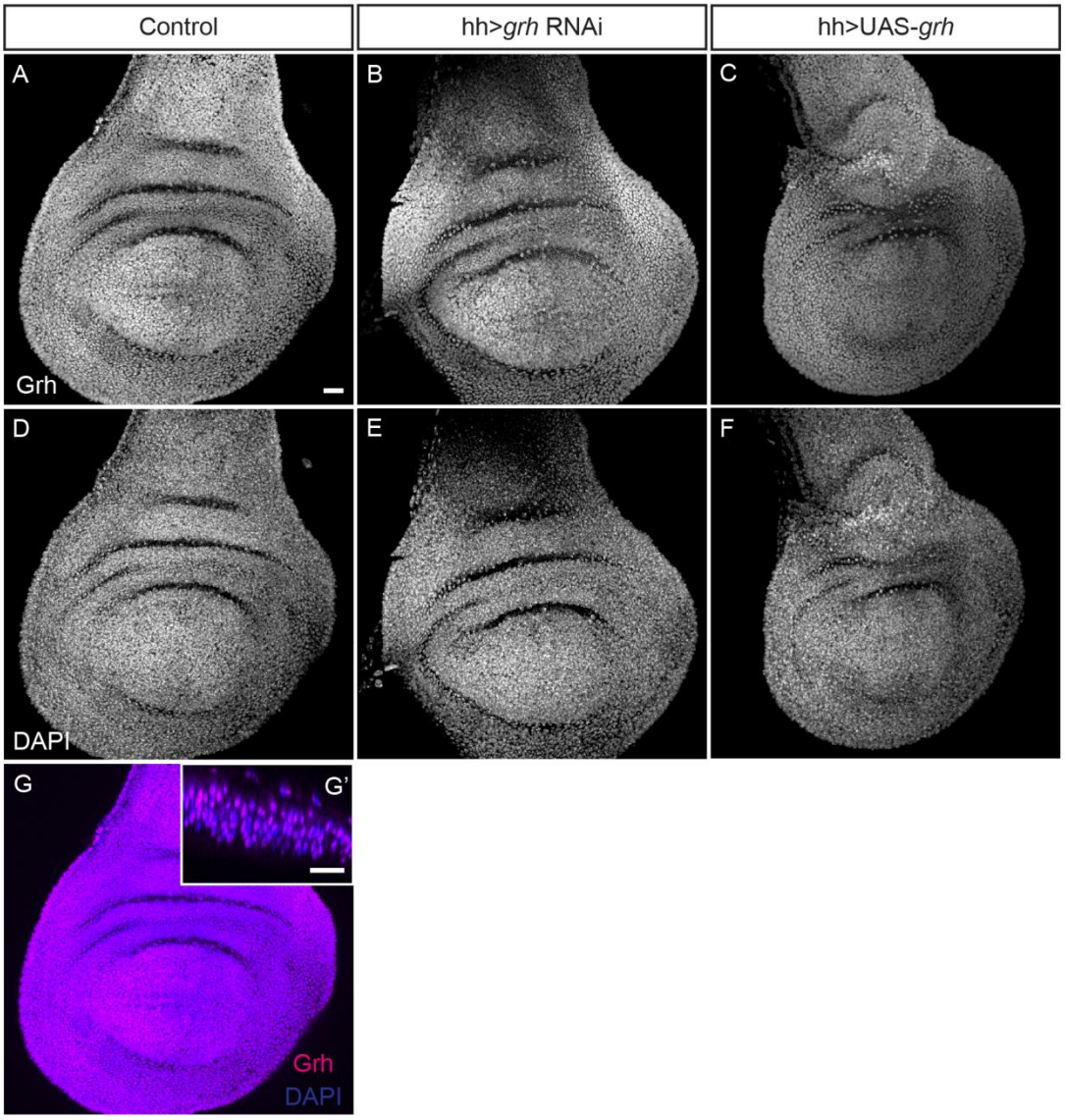

Figure 3.2. Grh protein localization in the wing imaginal disc. (A-C) Grh localization in control (w^{1118}/+; tubPGal80^{ts}/+; *hh*-Gal4, UAS-GFP/+) (A), *grh* knockdown (*grh* RNAi/tubPGal80^{ts}; *hh*-Gal4, UAS-GFP/+) (B) and *grh* overexpression (tubPGal80^{ts}/+; *hh*-Gal4, UAS-GFP/UAS-*grh*) (C) mid-L3 wing discs. (D-F) DAPI staining in control (D), *grh* knockdown (E) and *grh* overexpression (F) wing discs. (G) Merge of Grh and DAPI staining marks the cell nucleus in control wing discs. (A-G) are maximum Z projections. (G') X-Z section of the wing pouch in the control wing disc shown in G. Scale bars=20 µm.

In order to understand the role of *grh* in wing growth control, we first analysed the expression of *grh* in the larva wing imaginal disc, at the protein level, using an antibody against the *Drosophila* Grh (kindly supplied by C. Samakovlis).

In control wing discs, we observed that Grh is present in the entire wing disc (Fig. 3.2, A), being localized in the cell nucleus (Fig. 3.2, G-G').

Next we took advantage of this antibody to validate the genetic tools used to manipulate Grh expression. When we kept the flies at Gal4 restrictive temperature (18ºC) to ensure that the *grh* RNAi and UAS-*grh* constructs were not expressed, as expected, Grh levels in the control, *grh* RNAi or UAS-*grh* conditions were similar (Fig. 3.2 A-C). We then induced *grh* overexpression and knockdown by incubating the flies at permissive temperature (Fig. 3.3 and 3.4). After 12 h of *grh* knockdown (Fig. 3.3, B) we observed a partial reduction of Grh in the posterior compartment when compared to the control anterior compartment. In some wing discs the reduction in Grh levels was more evident than in others, likely reflecting variability in *grh* RNAi efficiency. With 24 h of *grh* RNAi expression (Fig. 3.4, B) we observed only negligible levels of Grh in the posterior compartment, suggesting a robust knockdown was achieved. After 48 h and 72 h of *grh* knockdown, the results were similar to 24 h (data not shown).

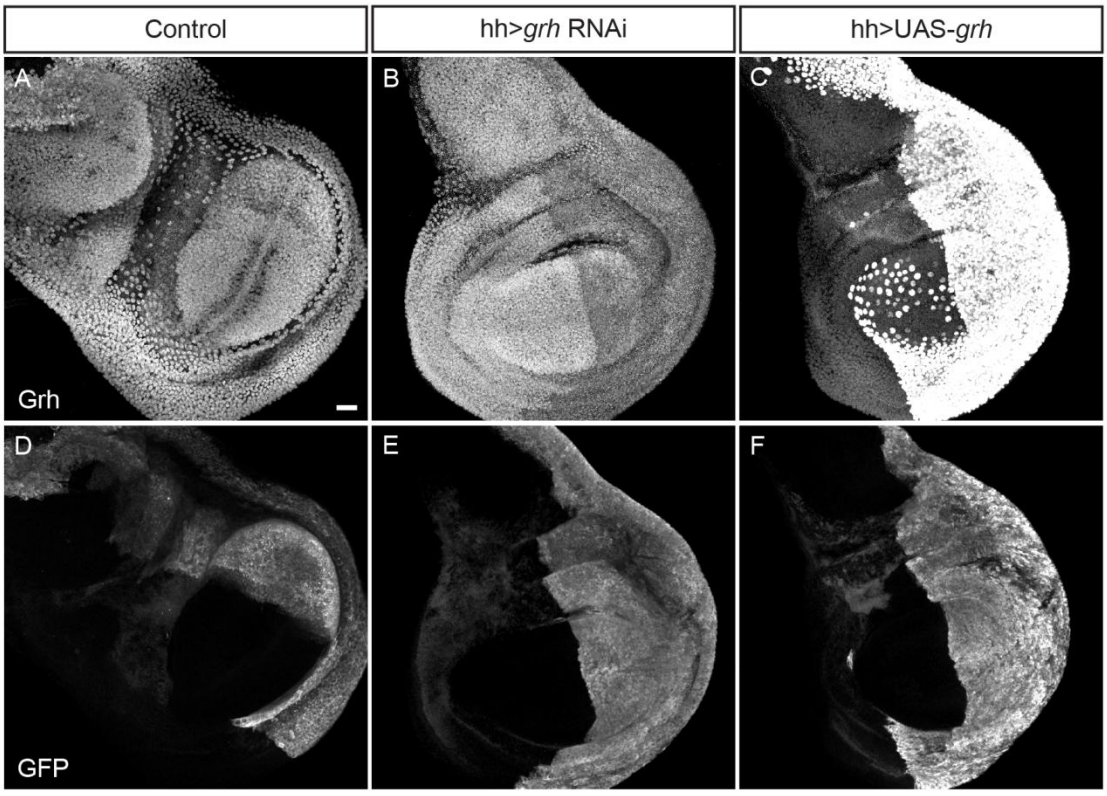

Figure 3.3. Grh expression pattern after 12 h of *grh* expression manipulation. (A-C) Expression pattern of Grh in control (w^{1118}/+; tubPGal80^{ts}/+; *hh*-Gal4, UAS-GFP/+) (A), *grh* knockdown (*grh* RNAi/tubPGal80^{ts}; *hh*-Gal4, UAS-GFP/+) (B) and *grh* overexpression (tubPGal80^{ts}/+; *hh*-Gal4, UAS-GFP/UAS-*grh*) (C) mid-L3 wing discs. (D-F) GFP staining marks the posterior compartment where *grh* RNAi/UAS-*grh* is expressed. Images are maximum Z projections. Scale bar=20 µm.

In the UAS-*grh* condition, after 12 h of expression (Fig. 3.3, C) Grh levels were clearly increased in the posterior compartment, compared with the anterior compartment. This phenotype was consistent in all the wing discs imaged. 24 h of *grh* overexpression (Fig. 3.4, C) led to a greater increase in Grh levels and consequently to defects in wing disc development. Wing discs were smaller than controls, mainly because of the great reduction in size of the posterior compartment.

These results show that we can successfully modulate Grh expression in a time and space-restricted manner in the wing disc.

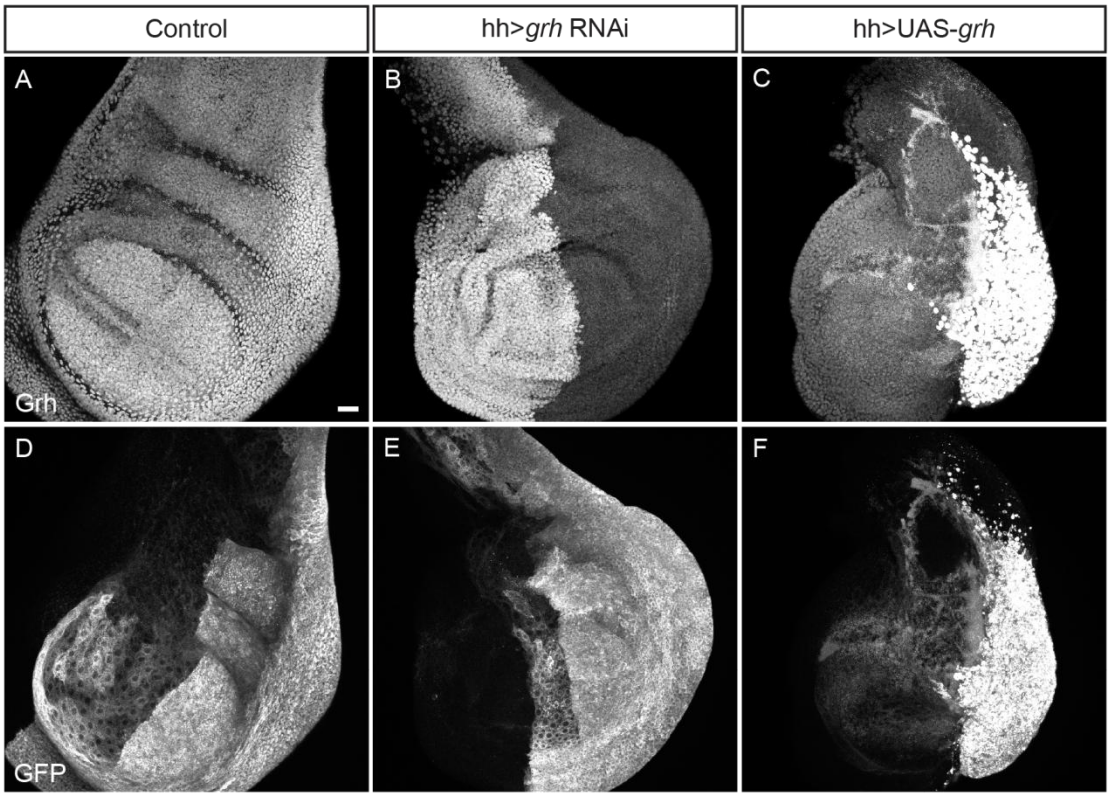

Figure 3.4. Grh expression pattern after 24 h of *grh* expression manipulation. (A-C) Expression pattern of Grh in control (w^{1118}/+; tubPGal80^{ts}/+; *hh*-Gal4, UAS-GFP/+) (A), *grh* knockdown (*grh* RNAi/tubPGal80^{ts}; *hh*-Gal4, UAS-GFP/+) (B) and *grh* overexpression (tubPGal80^{ts}/+; *hh*-Gal4, UAS-GFP/UAS-*grh*) (C) mid-L3 wing discs. (D-F) GFP staining marks the posterior compartment where *grh* RNAi/UAS-*grh* is expressed. Images are maximum Z projections Scale bar=20 µm.

3.3. Grh regulates apoptosis

3.3.1. *grh* misexpression promotes apoptosis

The third-instar larva wing disc is a highly proliferative tissue and, in normal conditions, apoptosis is almost inexistent (Milán *et al*., 1997). Our previous results showed that *grh* overexpression led to smaller wing discs. This phenotype could be due to reduced cell proliferation or activation of cell death. To uncover whether Grh induces apoptosis, we stained the wing discs with an antibody for activated caspase-3 (Casp3*) that detects apoptotic cells. Caspase-3 is a mammalian effector caspase, recognized as a key player in the degradation of cell material that happens during apoptosis (Nicholson *et al*., 1995).

Regarding *grh* knockdown, we observed apoptotic cells at 48 h (Fig. 3.6, B) but not at 12 h (Fig. 3.5, B), indicating that apoptosis is only induced when there is a strong *grh* knockdown. Besides being positive for Casp3*, these cells presented fragmented nuclei (Fig. 3.6, H), which is also a characteristic of dying cells.

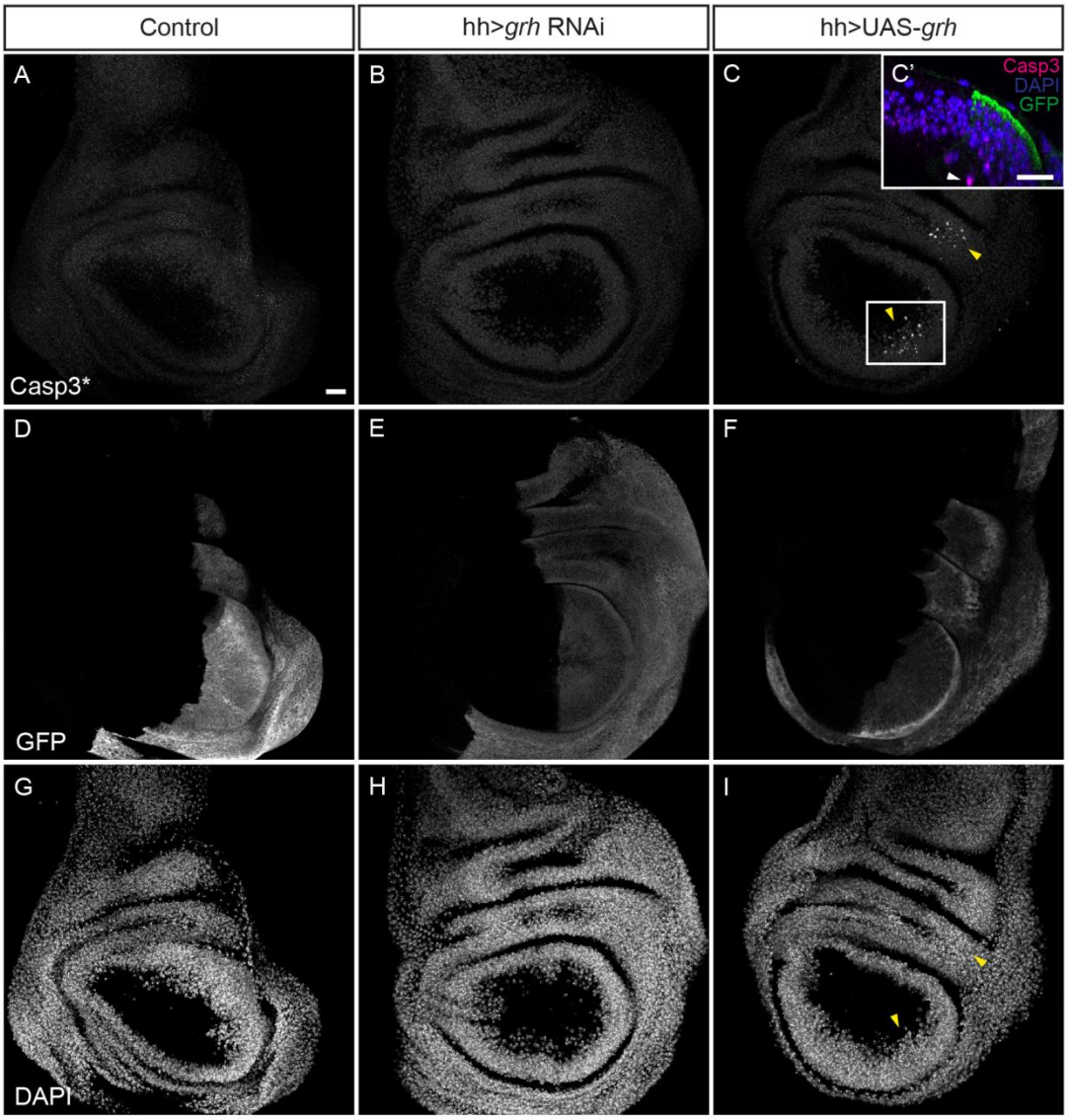

Figure 3.5. Apoptosis after 12 h of *grh* expression manipulation. (A-C) Casp3* staining in control (w^{1118}/+; tubPGal80^{ts}/+; *hh*-Gal4, UAS-GFP/+) (A), *grh* knockdown (*grh* RNAi/tubPGal80^{ts}; *hh*-Gal4, UAS-GFP/+) (B) and *grh* overexpression (tubPGal80^{ts}/+; *hh*-Gal4, UAS-GFP/UAS-*grh*) (C) mid-L3 wing discs. Images are partial maximum Z projections of the wing disc. (C') X-Z section of the region delimited by the white rectangle in C. White arrowhead points to a Casp-3* positive cell undergoing delamination. (D-F) GFP staining in the posterior compartment marks where *grh* RNAi/UAS-*grh* is expressed. (G-I) DAPI staining marks the cell nucleus. Yellow arrowheads point to Casp3* positive cells. Scale bars=20 µm.

When we overexpressed *grh* for 12 h we observed cells undergoing apoptosis in the posterior compartment (Fig. 3.5, C). These caspase-3-positive cells seemed to be extruded from the epithelium (Fig. 3.5, C'). At 48 h of overexpression the number of apoptotic cells increased while the wing disc size decreased (Fig. 3.6, C). This size reduction of the posterior compartment likely influenced tissue shape as these wing discs developed more folds than control wing discs.

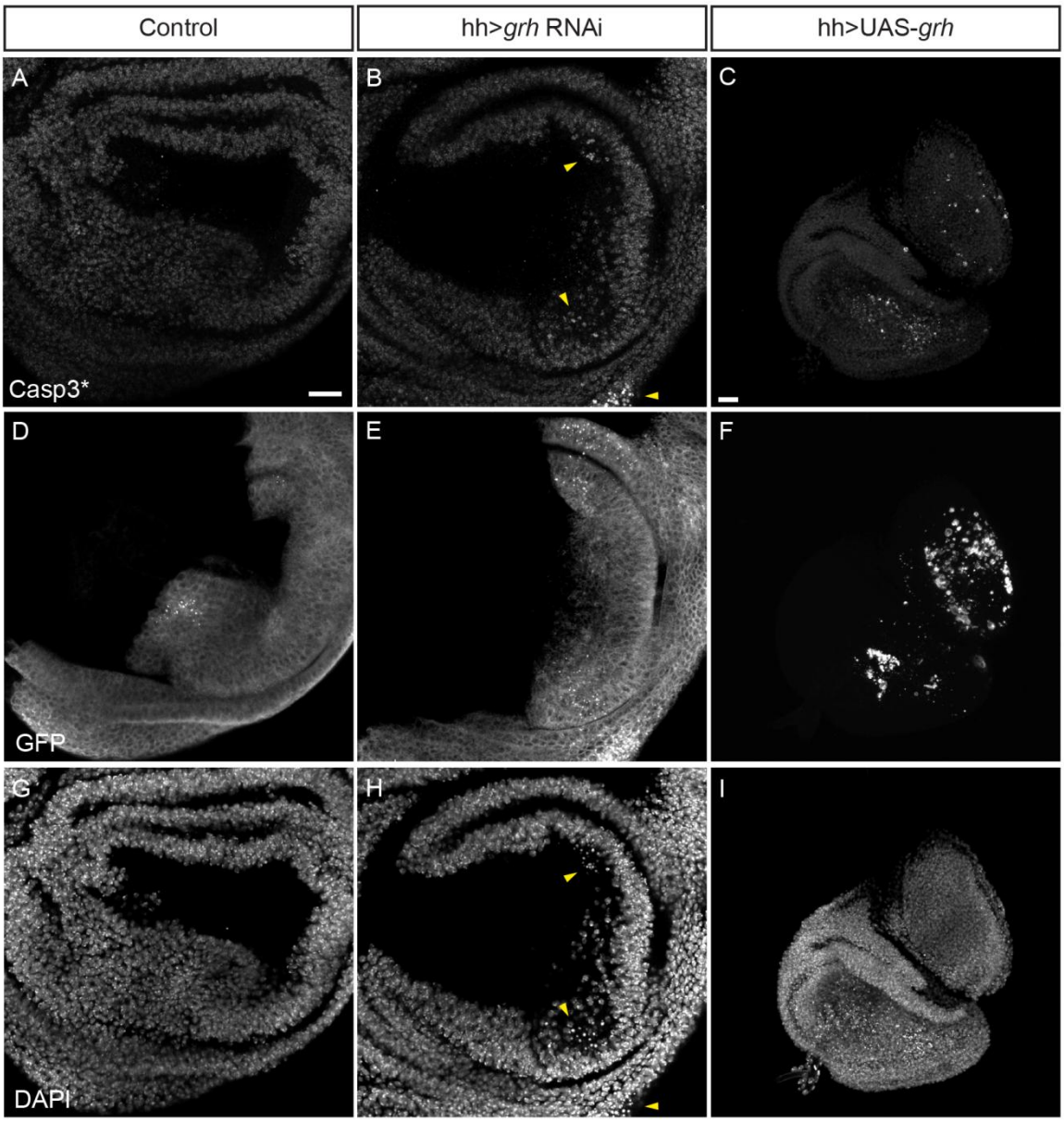

Figure 3.6.. Apoptosis after 48 h of *grh* expression manipulation. (A-C) Casp3* staining in control (w^{1118}/+; tubPGal80^{ts}/+; *hh*-Gal4, UAS-GFP/+) (A), *grh* knockdown (*grh* RNAi/tubPGal80^{ts}; *hh*-Gal4, UAS-GFP/+) (B) and *grh* overexpression (tubPGal80^{ts}/+; *hh*-Gal4, UAS-GFP/UAS-*grh*) (C) mid-L3 wing discs. (D-F) GFP staining in the posterior compartment marks where *grh* RNAi/UAS-*grh* is expressed. (G-I) DAPI staining marks the nucleus. Yellow arrowheads point to Casp3* positive cells. Images are partial maximum Z projections of the wing disc. Scale bar=20 μm.

3.3.2.*grh* knockdown activates JNK signalling

Our previous results showed that both *grh* knockdown and overexpression lead to apoptosis. JNK signaling pathway is associated with stress-induced apoptosis in *Drosophila* and mammals (reviewed by Dhanasekaran and Reddy 2008), so we investigated whether JNK was involved in the observed phenotype. To do so, we detected the expression of the *puckered* (*puc*) gene, a downstream target of JNK signaling (Martín-Blanco *et al*., 1998). We used the *puc*^{E69} allele, a previously used P

lacZ enhancer-trap line inserted in the *puc* gene that allows us to detect its expression by staining for β-galactosidase (β-gal, the product of the *lacZ* gene) (Ring and Martinez Arias, 1993).

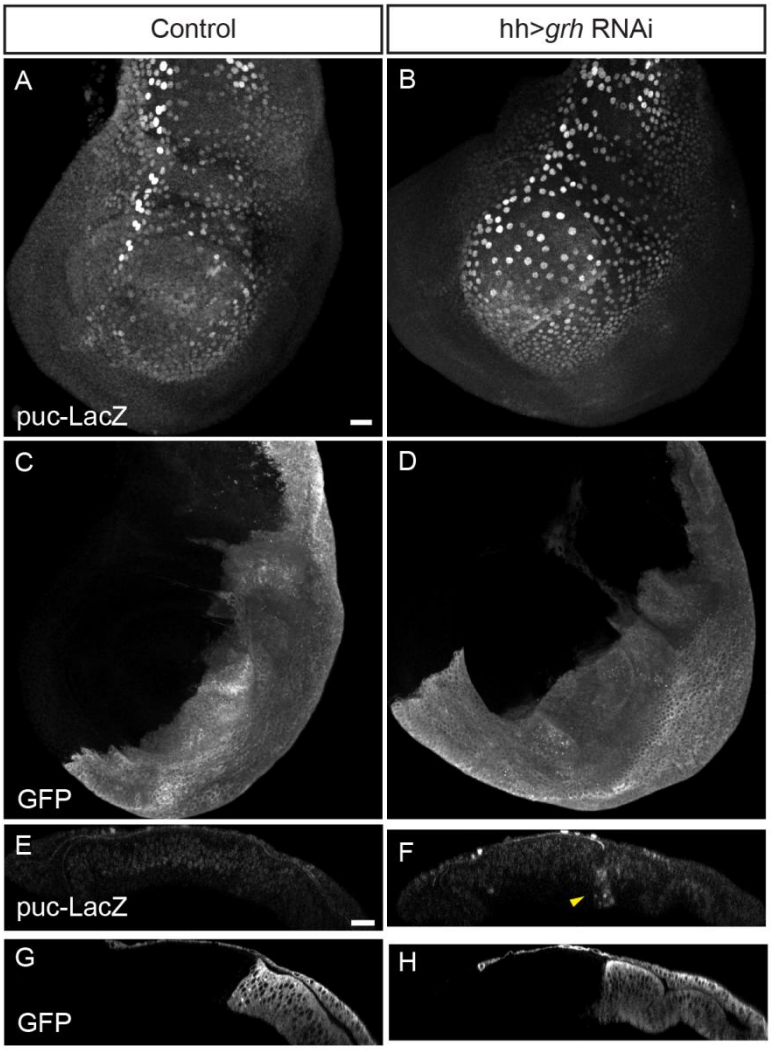

Figure 3.7. JNK signaling activation after 72 h of *grh* expression manipulation. (A-B) *puc-LacZ* staining in control (w^{1118}/+; tubPGal80^{ts}/+; *hh*-Gal4, UAS-GFP/+) (A) and *grh* knockdown (*grh* RNAi/tubPGal80^{ts}; *hh*-Gal4, UAS-GFP/+) (B) mid-L3 wing discs. (C-D) GFP staining in the posterior compartment marks where *grh* RNAi is expressed. Images are maximum Z projections. (E-H) X-Z sections of the wing pouch. Yellow arrowhead points to a group of *puc-LacZ* positive cells at the anterior-posterior boundary. Scale bars=20 μm.

Due to fly genetics and time constraints, we only analysed the wing disc phenotype after 72 h of *grh* RNAi expression (Fig. 3.7, B). We observed ectopic *puc* expression in the posterior compartment, localized close to the anterior-posterior boundary (Fig. 3.7, F). These cells seemed to be delaminating from the tissue, which suggests that they are undergoing cell death.

In summary, our results show that both *grh* knockdown and overexpression induce apoptosis in the wing disc and that JNK signaling is activated upon *grh* knockdown, suggesting that Grh regulates apoptosis.

3.4. Grh regulates cell proliferation

3.4.1. *grh* knockdown and overexpression have opposite effects on cell proliferation

Another way of regulating tissue growth is through cell proliferation. To understand whether Grh regulates cell proliferation we detected mitotic cells by staining the wing discs with an antibody for Phospho-Histone-H3 (PH3) (Hendzel *et al*., 1997).

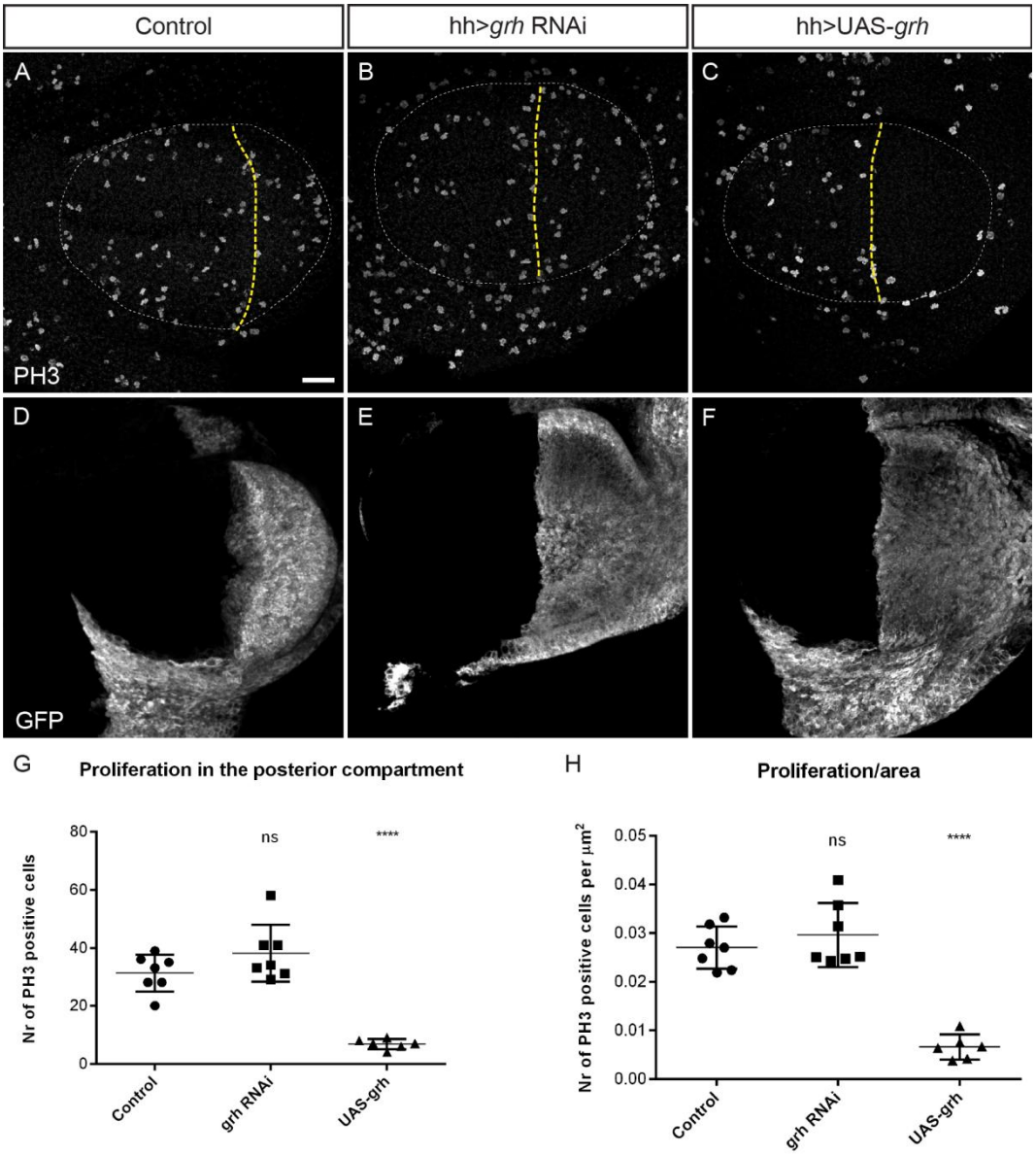

Figure 3.8. Cell proliferation after 12 h of *grh* expression manipulation. (A-C) PH3 staining in control (w^{1118}/+; tubPGal80^{ts}/+; *hh*-Gal4, UAS-GFP/+) (A), *grh* knockdown (*grh* RNAi/tubPGal80^{ts}; *hh*-Gal4, UAS-GFP/+) (B) and *grh* overexpression (tubPGal80^{ts}/+; *hh*-Gal4, UAS-GFP/UAS-*grh*) (C) mid-L3 wing discs. White dashed line outlines the wing pouch. Yellow dashed line represents the anterior-posterior boundary. Anterior is left and posterior is right. (D-F) GFP staining in the posterior compartment marks where *grh* RNAi/UAS-*grh* is expressed. All images are maximum Z projections. Scale bar=20 µm. (G,H) Graphs showing the number of PH3 positive cells (G) and the number of PH3 positive cells per area (H) in the posterior compartment in control, *grh* RNAi and UAS-*grh* wing discs. *grh* overexpressing wing discs show a significant reduction in the number of PH3-positive cells (G) and PH3-positive cells per area (µm^2) (H) in the posterior compartment compared to control wing discs. *grh* RNAi show no differences in the number of mitotic cells compared to controls. Student's t-test was used to determine statistic significance (**** p<0.0001). ns=not significant. Error bars represent standard deviations. Control n=7, *grh* RNAi n=7, UAS-*grh* n=6.

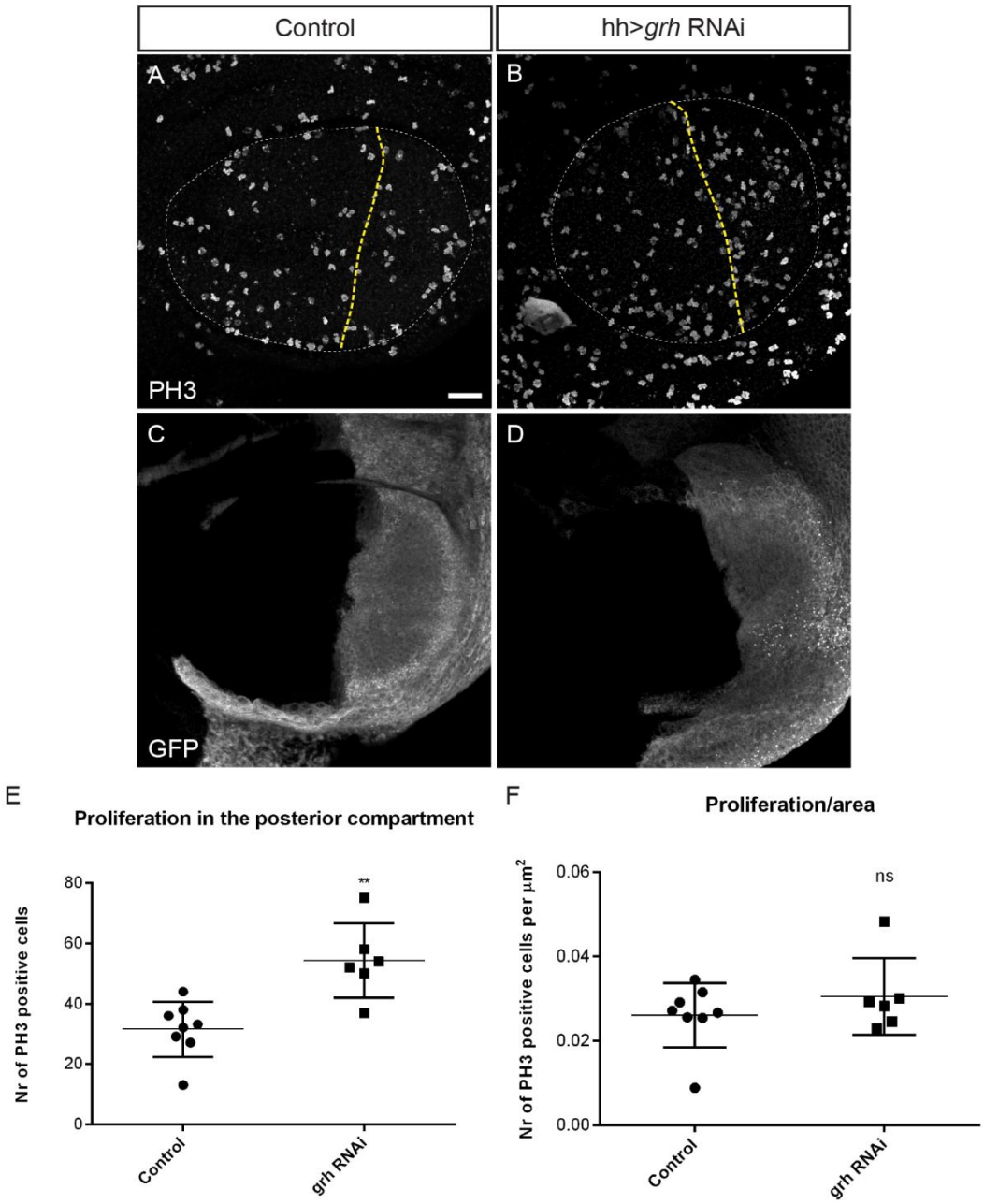

Figure 3.9. Cell proliferation after 72 h of *grh* expression manipulation. (A-B) PH3 staining in control (w^{1118}/+; tubPGal80^{ts}/+; *hh*-Gal4, UAS-GFP/+) (A) and *grh* knockdown (*grh* RNAi/tubPGal80^{ts}; *hh*-Gal4, UAS-GFP/+) (B) mid-L3 wing discs. White dashed line outlines the wing pouch. Yellow dashed line represents the anterior-posterior boundary. (C-D) GFP staining in the posterior compartment marks where *grh* RNAi is expressed. Images are maximum Z projections. Anterior is left and posterior is right. Scale bar=20 µm. (E-F) Graphs showing the number of PH3 positive cells (G) and the number of PH3 positive cells per area (H) in the posterior compartment in control and *grh* RNAi wing discs. *grh* knockdown wing discs show a significant increase in the number of PH3-positive cells but not in the number PH3-positive cells per area (µm^2) in the posterior compartment, compared to control wing discs. Student's t-test was used to determine statistic significance. (**p=0.0018). Ns=not significant. Error bars represent standard deviations. Control n=8, *grh* RNAi n=6.

After 12 h of *grh* knockdown we observed only a slight, not significant, difference in the number of PH3-positive cells in the posterior compartment when compared to controls (Fig. 3.8, A-B, G-H). However, after 72 h of *grh* RNAi expression we detected a significant increase in the number of mitotic cells (Fig. 3.9, A, C, E). This activation of cell proliferation was accompanied by an increase in

posterior compartment area. These two parameters seem to have increased in a proportional manner in the *grh* knockdown, because the number of mitotic cells per area (μm^2) was not significantly different from control wing discs (Fig. 3.9, F).

When we overexpressed *grh* for 12 h we observed a significant decrease in the PH3-positive cells in the posterior compartment when compared with control wing discs (Fig. 3.8, A, C, G). Furthermore, we detected a significant decrease in the number of proliferating cells per area, indicating that the area of the posterior compartment remained similar to the controls (Fig. 3.8, H).

Our results show that *grh* knockdown induces an increase in the number of mitotic cells while *grh* overexpression has the opposite effect in the wing disc, thus pointing to a role of Grh in cell proliferation.

3.4.2. Grh does not seem to regulate the Hippo pathway

First discovered in *Drosophila*, the Hippo signaling pathway has been shown to be involved in the control of proliferation, apoptosis, differentiation, and migration, being a key regulator of organ size during developmental growth. Mutations that lead to dysfunctional Hippo pathway signaling induce dramatic tissue overgrowth (reviewed in Staley and Irvine, 2012).

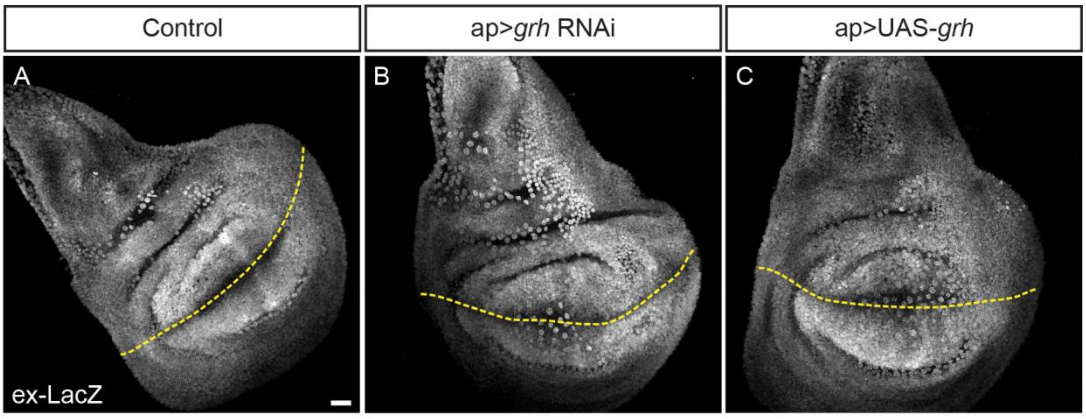

Figure 3.10 *expanded* (*ex*) expression pattern after 16 h of *grh* expression manipulation. (A-C) *ex-LacZ* staining in control (*ap*-Gal4,*ex-LacZ*/tubPGal80^{ts}) (A), *grh* knockdown (*ap*-Gal4,*ex-LacZ*/*grh* RNAi; tubPGal80^{ts}/+) (B) and *grh* overexpression (*ap*-Gal4,*ex-LacZ*/tubPGal80^{ts}; UAS-*grh*/+) (C) mid-L3 wing discs. *grh* RNAi and UAS-*grh* were expressed under the control of the *ap* promoter, which is expressed in the dorsal compartment of the wing disc. Yellow dashed line represents the dorsal-ventral boundary. Dorsal is up, ventral is down. Images are maximum Z projections. Scale bar=20 µm.

As we found that Grh regulates both apoptosis and proliferation in the wing disc, we tested whether Grh regulates the Hippo pathway. We used a previously described *LacZ* reporter line for the gene *expanded* (*ex*), a bona fide target of this pathway (Hamaratoglu *et al*., 2006). Both knockdown and *grh* overexpression induced no changes in *expanded* expression in the wing disc after 16 h of *grh* manipulation (Fig. 3.10). We also tested 24 h, 48 h and 72 h and obtained similar results (data not shown).

Based on the results obtained with this reporter, Grh does not seem to regulate the Hippo pathway.

3.5. Grh regulates wing size

Our experiments show that Grh significantly influences the growth of the developing wing disc by regulating both proliferation and apoptosis. Therefore, we asked whether these developmental defects have an impact in the adult wing.

To assess the effect of *grh* knockdown or overexpression specifically during wing disc growth stages, we expressed either *grh* RNAi or UAS-*grh* only during larval stages and then measured the anterior and posterior area of the adult wings.

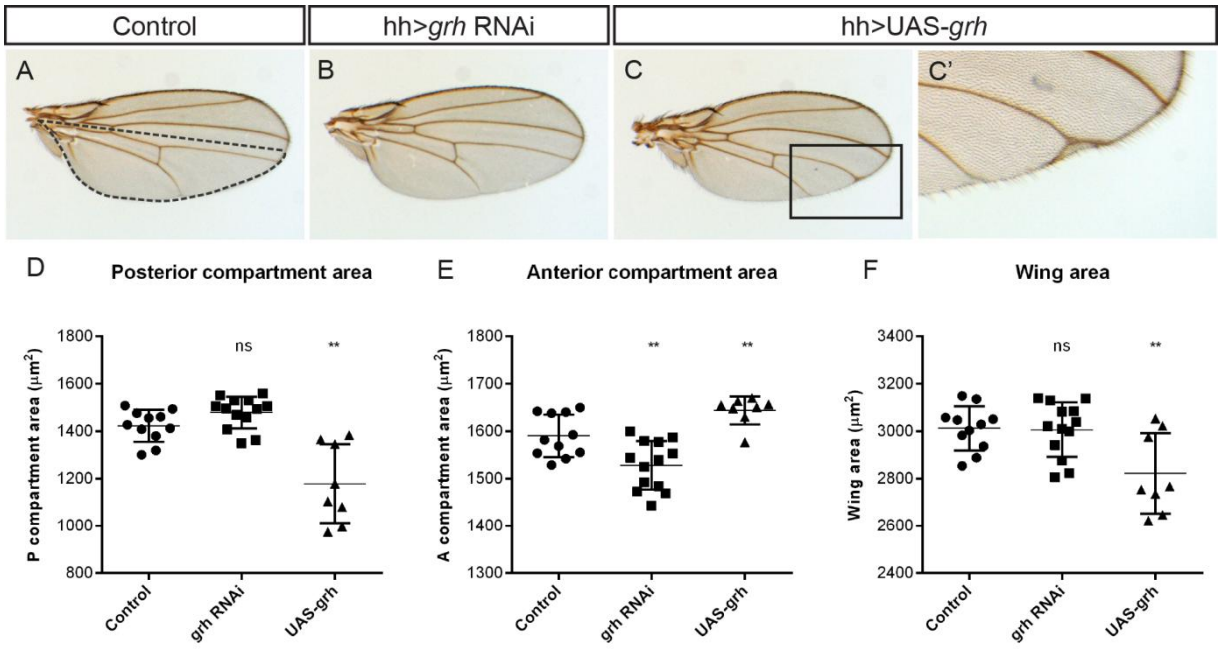

Figure 3.11. Wing area after 12 h of *grh* expression manipulation. (A-C) Adult wings from control (w^{1118}/+; tubPGal80^{ts}/+; *hh*-Gal4, UAS-GFP/+) (A), *grh* knockdown (*grh* RNAi/tubPGal80^{ts}; *hh*-Gal4, UAS-GFP/+) (B) and *grh* overexpression (tubPGal80^{ts}/+; *hh*-Gal4, UAS-GFP/UAS-*grh*) (C) flies. Black dashed line in A represents the posterior compartment (C') Zoom of the region delimited by the black rectangle in C, depicting wing vein defects upon *grh* overexpression. Scale bar=500 µm. (D-E) Graphs showing the area of the posterior compartment of the adult wing (D) and total wing area (E) in controls, *grh* RNAi and UAS-*grh*. *grh* overexpressing wings show a significant reduction in the posterior compartment area (D, **p=0.0039) and in the total wing area (F, **p=0.0060), and an increase in anterior compartment area (E, **p=0.0093) compared to control wings. *grh* RNAi wings show a significant increase in anterior compartment area (E, **p=0.0051), whereas posterior compartment and total wing areas are similar to control wings (D, F, ns=not significant). Student's t-test was used to determine statistical significance. Error bars represent standard deviations. Control n=11, *grh* RNAi n=13, UAS-*grh* n=8.

Regarding the *grh* overexpression, we observed a significant decrease in the posterior area of the wing when compared to control wings (Fig. 3.11, A, C, D). In contrast, the anterior compartment was (slightly) increased (Fig. 3.11, E). Together this lead to a reduction in the total wing area (Fig. 3.11, F). We also noticed wing vein defects in the posterior compartment such as ectopic veins or bifurcations. (Figure 3.11, C').

When we knocked-down *grh* for 12 h we observed no significant difference in the posterior compartment and total wing area when compared to control wings (Fig. 3.11, A, B, D, F), although there was a decrease in the anterior compartment area (Fig. 3.11, E). After 24 h of *grh* RNAi expression (Fig. 3.12) we observed two different phenotypic classes. About 40% of the wings showed normal patterning (Fig. 3.12, B), while the other 60% were curved, and presented wing vein defects

and abnormal pigmentation (Fig. 3.12, C-C'). Because of these shape defects we could only quantify the area in wings of the first phenotypic class (Fig. 3.12, B). Surprisingly, *grh* knockdown induced smaller wings (Fig. 3.12, A, B, F). Not only the posterior compartment was significantly smaller than in controls, but the anterior compartment also followed that tendency (Fig. 3.12, D, E).

Our results reveal that Grh influences final adult wing size and that both *grh* knockdown and overexpression result in smaller wings.

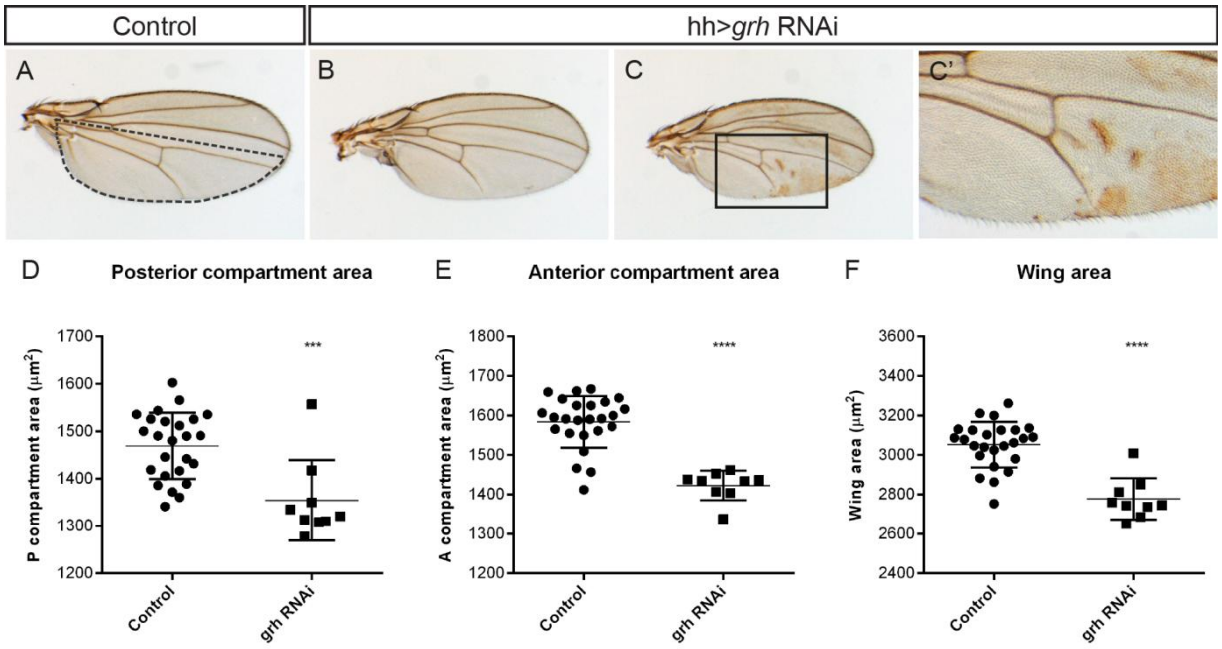

Figure 3.12. Wing area after 24 h of *grh* expression manipulation. (A-C) Adult wings from control (w^{1118}/+; tubPGal80^{ts}/+; *hh*-Gal4, UAS-GFP/+) and *grh* knockdown (*grh* RNAi/tubPGal80^{ts}; *hh*-Gal4, UAS-GFP/+) flies. B and C represent two phenotypic classes of *grh* knockdown. Black dashed line in A represents the posterior compartment (C') Zoom of the region delimited by the black rectangle in C, depicting wing vein defects and abnormal pigmentation. Scale bar=500 µm. (D) *grh* knockdown wings show a significant reduction in the posterior compartment area (D, *** p=0.0004), anterior compartment area (E, ****p<0.0001) and in the total wing area (F, ****p<0.0001), compared to control wings. Only the wings from phenotypic class represented in B were measured. Student's t-test was used to determine statistical significance. Error bars represent standard deviations. Control n=25, *grh* RNAi n=9.

3.6. Grh regulates E-cadherin

E-cadherin is a calcium-dependent cell-cell adhesion molecule with a crucial role in cell adhesion, cell polarity and differentiation (reviewed by van Roy and Berx, 2008). In addition, changes in E-cadherin expression have been implicated in tumor progression and invasion (reviewed by Stemmler, 2008). Grh has been implicated in the regulation of E-cadherin in both *Drosophila* and mice (Almeida and Bray, 2005; Werth *et al*., 2010). Moreover, downregulation of Grhl2 in breast cancer is accompanied by loss of E-cadherin and gain of N-cadherin, resulting in epithelial-to-mesenchymal transition (Cieply *et al*., 2012). For all these reasons, we wanted to understand whether Grh regulates E-cadherin levels in the wing disc.

At 12 h of *grh* RNAi expression, wing discs presented higher levels of E-cadherin in the posterior compartment than in the control anterior compartment (Fig. 3.13, B). The severity of this phenotype varied depending on the wing disc, which might be related to the observed variability in Grh protein localization after 12 h of *grh* knockdown.

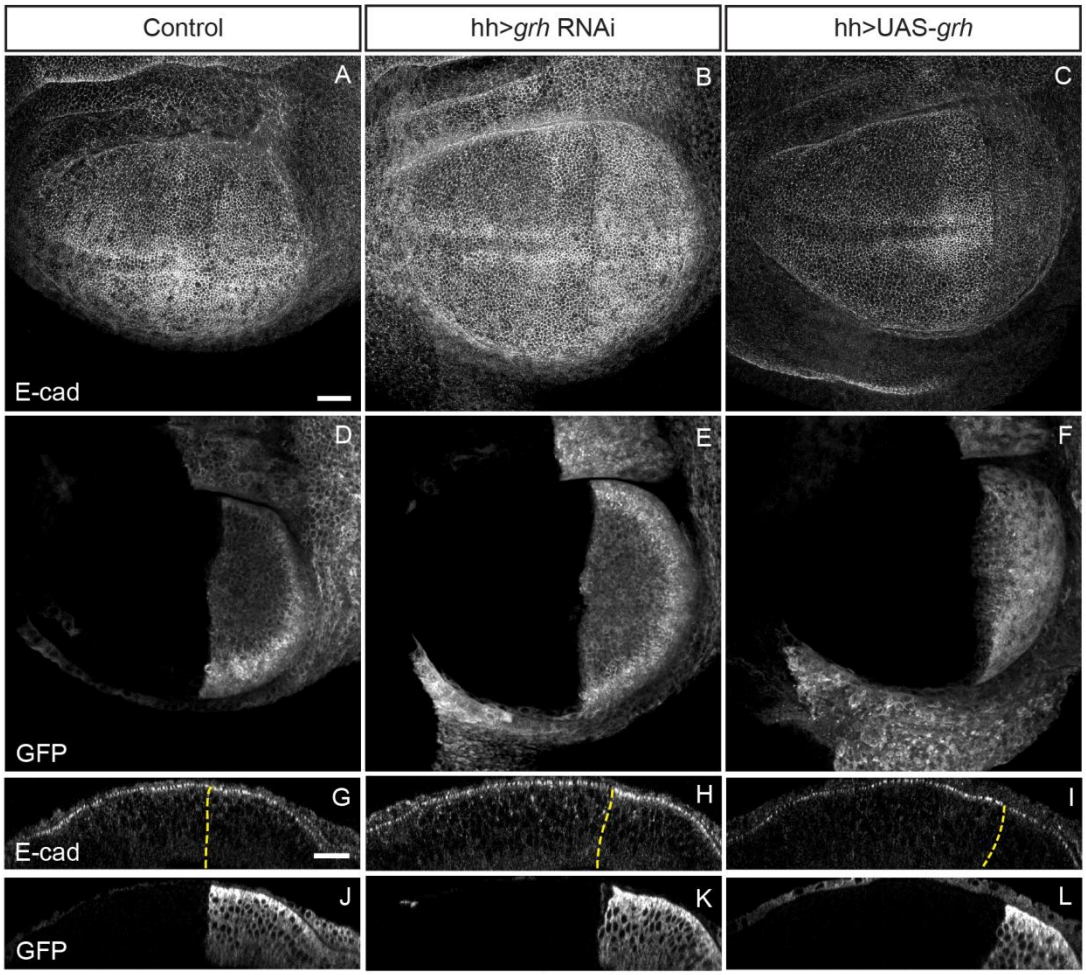

Figure 3.13. E-cadherin levels and localization after 12 h of *grh* expression manipulation. (A-C,G-I) E-cadherin staining in control (w^{1118}/+; tubPGal80^{ts}/+; *hh*-Gal4, UAS-GFP/+) (A,G), *grh* knockdown (*grh* RNAi/tubPGal80^{ts}; *hh*-Gal4, UAS-GFP/+) (B,H) and *grh* overexpression (tubPGal80^{ts}/+; *hh*-Gal4, UAS-GFP/UAS-*grh*) (C,I) mid-L3 wing discs. (D-F,J-L) GFP staining in the posterior compartment marks where *grh* RNAi/UAS-*grh* is expressed. (A-F) Images are maximum Z projections. (G-L) X-Z sections of the wing pouch. Yellow dashed line in G-I represents the anterior-posterior boundary. Anterior is left and posterior is right. Scale bars=20 µm.

When we knocked-down *grh* for 72 h we observed higher levels of E-cadherin compared to controls, not only in the posterior compartment, but in the whole wing disc (Fig. 3.14, B). This suggests that *grh* knockdown induces a non-cell autonomous response.

We also looked at E-cadherin localization on X-Z sections of the wing pouch. We observed that in the *grh* RNAi condition, E-cadherin localized not only to the apical domain of the cells as in the controls, but also in accumulations on the lateral membrane of cells, both in the anterior and in the posterior compartment of the wing disc (Fig. 3.13, H; Fig. 3.14, H).

On the other hand, when we overexpressed *grh*, we detected less E-cadherin in the posterior compartment when compared to controls (Fig. 3.13, C). In the X-Z sections we observed that E-cadherin was apically localized as in the controls (Fig. 3.13, I).

These results suggest that Grh might inhibit E-cadherin expression in the wing disc. Furthermore, Grh seems to regulate E-cadherin localization in epithelial cells.

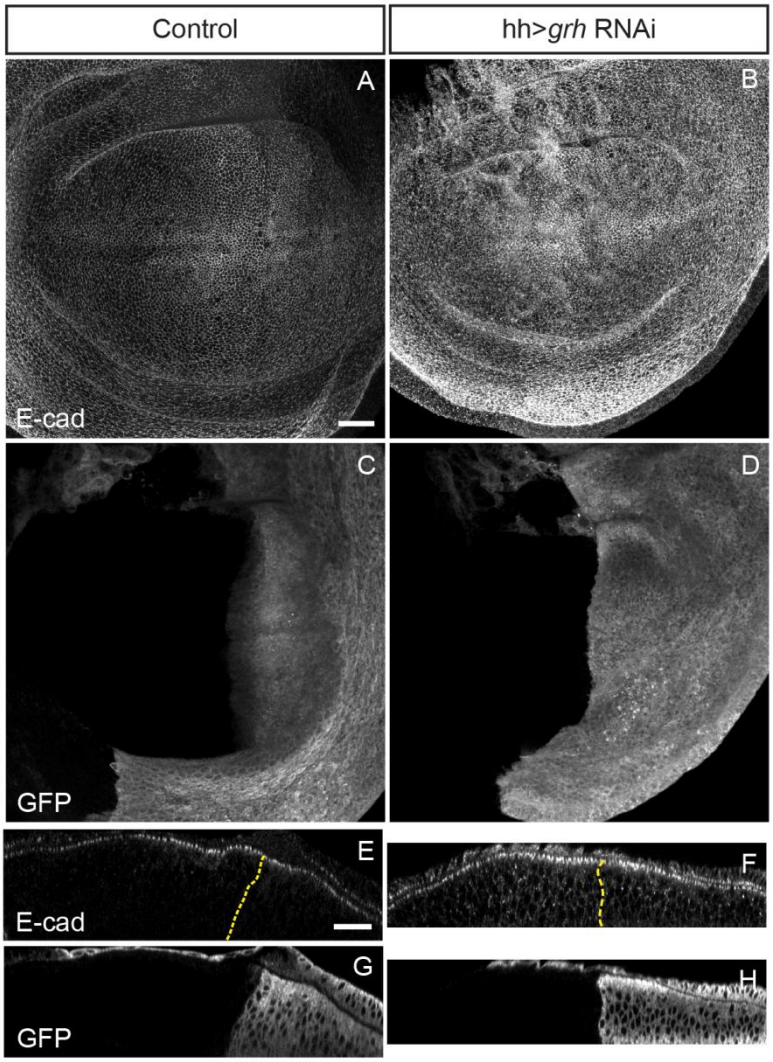

Figure 3.14. E-cadherin levels and localization after 72 h of *grh* expression manipulation. (A-B,E-F) E-cadherin staining in control (w^{1118}/+; tubPGal80^{ts}/+; *hh*-Gal4, UAS-GFP/+) (A,E) and *grh* knockdown (*grh* RNAi/tubPGal80^{ts}; *hh*-Gal4, UAS-GFP/+) (B,F) mid-L3 wing discs. (C-D,G-H) GFP staining in the posterior compartment marks where *grh* RNAi is expressed. (A-D) Maximum Z projections of the wing disc. (E-H) X-Z sections of the wing pouch. Yellow dashed line represents the anterior-posterior boundary. Anterior is left, posterior is right. Scale bars=20 µm.

3.7. Grh seems to regulate actin levels

Filamentous actin (F-actin) is part of the cell cytoskeleton, thus influencing the mechanical properties and shape of cells, which are critical to their functions. F-actin is involved in numerous cell behaviors, such as morphology, movement, division, endocytosis, and intracellular trafficking (reviewed in Pollard and Cooper, 2009). It has also been shown that actin and the Hippo pathway are

interconnected in the control of tissue growth (reviewed in Matsui and Lai, 2013). Interestingly, a screen performed in *grh* mutant embryos revealed that several actin-binding proteins/regulators are Grh targets (Paré *et al*., 2012).

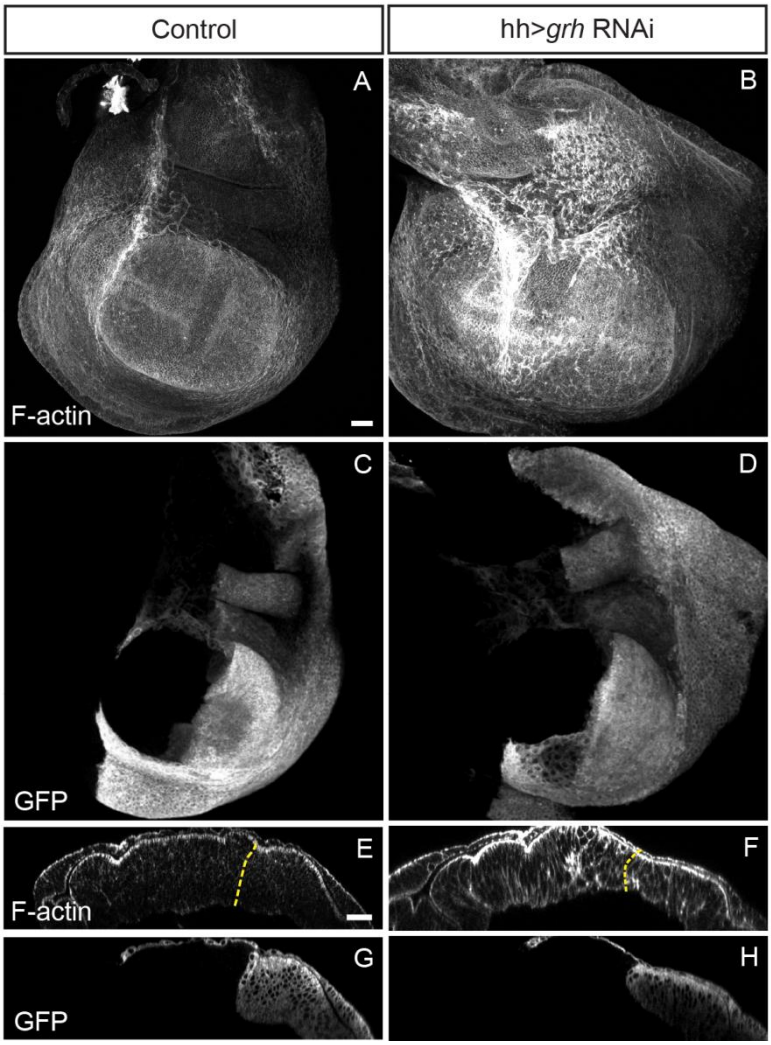

Figure 3.15. F-actin localization after 72 h of *grh* expression manipulation. (A-B, E-F) F-actin in control (w^{1118}/+; tubPGal80^{ts}/+; *hh*-Gal4, UAS-GFP/+) (A,E) and *grh* knockdown (*grh* RNAi/tubPGal80^{ts}; *hh*-Gal4, UAS-GFP/+) (B;F) mid-L3 wing discs. Images are maximum Z projections. (C-D) GFP staining in the posterior compartment marks where *grh* RNAi is expressed. (E-H) X-Z sections of the wing pouch. Yellow dashed line represents the anterior-posterior boundary. Anterior is left, posterior is right. Scale bars=20 µm.

To assess the effect of *grh* expression on actin levels we used fluorescently-labeled phalloidin, which selectively binds to F-actin (Faulstich *et al*, 1988).

Due to technical difficulties, we only assessed the phenotype at 72 h of *grh* RNAi expression. Here we observed an increase in F-actin, not only in the posterior compartment, but in the entire wing disc when compared to controls (Fig. 3.15, A-B, E-F). We also detected an effect on tissue shape in the *grh* RNAi expressing wing discs (compare Fig. 3.15, E and F). Interestingly, actin seemed to accumulate in the places where the tissue was affected by folds (Fig. 3.15, F).

These results suggest that Grh might have a role in the regulation of actin cytoskeleton dynamics during wing disc development.

3.8. Generation of *grh* mutant clones

Clonal analysis allows the analysis of mutations that are lethal when affecting the entire animal. In addition, it represents an invaluable tool for understanding cell lineage and cell interactions during development, along with many other applications (Perrimon, 1998). Since *grh* mutants die at the end of embryogenesis, we decided to establish this technique in wing imaginal discs to determine the effect of a complete deletion of the *grh* locus. For that we generated *grh* mutant clones in wing imaginal discs.

Using the FLP/FRT technique we generated *grh* mutant clones that are marked by the absence of GFP (Golic and Lindquist, 1989). We used a ubiquitously expressed heat-shock inducible FLP so that we could control the developmental stage at which we induced mitotic recombination and thus clone induction. After optimizing the heat-shock conditions, we performed the heat-shock when the larvae were in L1 stage and imaged them 3 days later (mid-L3 larvae) to allow growth of the mutant clones. To validate that the GFP-negative cells were indeed mutant for *grh*, we stained the wing discs with the Grh antibody (Fig. 3.16, B,E).

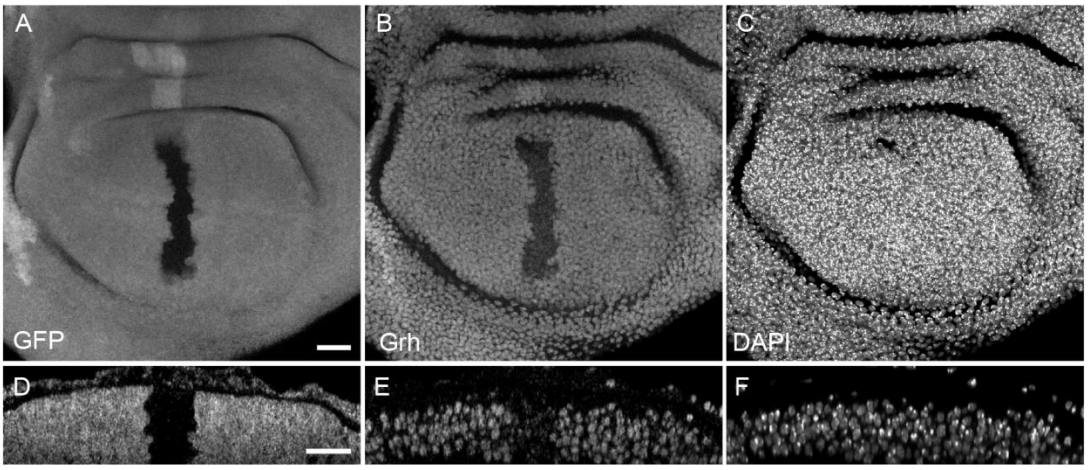

Figure 3.16 Generation of *grh* mutant clones. (A-F) Heterozygous wing disc with *grh* mutant homozygous clones marked by the absence of GFP. (A,D) GFP staining showing homozygous mutant clone lacking GFP and twin homozygous wild-type clones with higher GFP intensity.(B,E) Grh antibody staining showing lack of Grh protein in mutant clones and higher expression of Grh in twin clones. (C,F) DAPI staining shows cell nuclei. (A-C) Images are maximum Z projections. (D-F) X-Z sections of the wing pouch. Scale bars=20 µm.

In the wing discs where we detected the presence of *grh* mutant clones, the number of clones varied from one to three per disc. We observed that Grh was absent from GFP negative cells, indicating that mitotic recombination took place and generated homozygous *grh* mutant cells (Fig. 3.16 A-B, D-E). In rare cases we observed the twin (homozygous wild type) clones but not the mutant clones, suggesting that *grh* mutant cells may have died earlier.

Our results show that we can successfully generate *grh* mutant clones in the wing imaginal disc. Although in this project we were not able to analyse the phenotypes caused by the loss of *grh* in these clones, this technique will help understand the functions of Grh in the wing imaginal disc growth in future work.

4. DISCUSSION

4.1. Manipulating Grh in the wing disc

Grh is recognized for its critical role in epithelia development and maintenance. It is not surprising that the manipulation of its expression levels leads to severe effects in epithelia, which ultimately result in lethality. When we knocked down or overexpressed Grh using the MS1096-Gal4 driver, with which lethally was reduced and adult flies ecloded, we observed severe defects in wing growth and development. *grh* RNAi expressing wings were necrotic and UAS-*grh* overexpressing wings presented very small and abnormal wings. To minimize this effect we controlled *grh* expression in a temporal and tissue-specific manner. With this approach we were able to successfully knockdown and overexpress *grh* in the wing imaginal disc and investigate its role in the growth of this organ.

To analyze the effects of *grh* knockdown and overexpression at the protein level we used immunofluorescence stainings. We decided to use the *hh*-Gal4 driver, which drives gene expression only in the posterior compartment of the wing disc. This experimental assay allowed us to assess qualitative differences in protein levels and localization between the anterior and the posterior compartment, together with the comparison with control wing discs.

Our results revealed that 12 h of *grh* overexpression (UAS-*grh*) were sufficient to induce a phenotype without compromising fly development and survival, while *grh* knockdown using the RNAi technique required more time to efficiently reduce *grh* expression levels.

4.2. Regulation of tissue growth by Grh

We observed that both *grh* knockdown and overexpression lead to apoptosis, although the effects of overexpressing *grh* are more severe. Interestingly, we also observed ectopic activation of JNK signaling in the *grh* RNAi expressing wing discs. As it is known that this pathway can be activated in apoptotic cells (McEwen and Peifer, 2005), our results suggest that the lack of Grh might induce apoptosis through JNK signaling. JNK pathway can be activated by stress stimuli and then induce apoptosis (McEwen and Peifer, 2005), but it can also be activated as a consequence of the apoptosis pathway (Kondo *et al*., 2006). In addition, the outcome of JNK signaling can vary depending on the stimulus. For example, this signaling pathway also regulates cell migration (Pastor-Pareja *et al*., 2004; Llense and Martin-Blanco, 2008), and invasion (Igaki *et al*., 2006). Therefore, it would be interesting to investigate the mechanisms that lead to the activation of the JNK pathway in the absence of Grh and whether that is related to the observed apoptotic events or to other cellular processes.

We observed that while Grh overexpression leads to a striking reduction in the number of mitotic cells, *grh* knockdown has the opposite effect suggesting that Grh might regulate cell proliferation. To support this hypothesis, we observed an increase in the surface area of the posterior compartment in the absence of Grh. Another possibility is that Grh knockdown leads to a cell cycle arrest at the stage

where Histone H3 is phosphorylated (during mitosis) (Hans and Dimitrov, 2001). To clarify this we would need to analyze other markers of the cell cycle. The increase in area of the wing disc in the Grh knockdown could also be due to an increase in cell size. Although we did not quantify cell size, no major differences in cell size between the posterior and the anterior compartment or the control wing discs were noticeable, further supporting our hypothesis that Grh regulates cell proliferation in the wing disc.

In the wing disc, many signaling pathways regulate cell proliferation (Neto-Silva *et al.*, 2009). We tested whether the Hippo pathway was involved by looking at the expression pattern of one of its target genes, *expanded*. We detected no difference in *expanded* levels between the dorsal (where we expressed UAS-*grh* and *grh* RNAi) and the ventral compartment, which suggests that Grh does not regulate the Hippo pathway. It would be interesting to test other reporters of Hippo pathway activity to confirm this phenotype, but based on our results Grh seems to regulate cell proliferation through a different pathway.

Another question that we would like to address is the relationship between apoptosis and proliferation and how this is influenced by Grh. Apoptotic cells can induce mitogenic signaling, promoting proliferation of the surrounding cells (Ryoo *et al*. 2004; Fan and Bergmann, 2008). Conversely, when overproliferation occurs, apoptosis is induced to restore cell number (Menéndez *et al*., 2010). So there is a tight regulation between these two processes that ensures normal tissue growth and development. One way of understanding the relationship between proliferation and apoptosis would be to inhibit apoptosis and observe the influence on cell proliferation.

Although in a completely different context, it was previously shown by Cenci and Gould (2005) that Grh can regulate both cell proliferation and apoptosis. This study on neuroblast development revealed that Grh differentially regulates thoracic and abdominal neuroblasts. In the thorax, Grh stimulates proliferation by maintaining neuroblasts in an active mitotic state, while in the abdomen Grh promotes apoptosis by regulating neuroblast competence to respond to Abdominal-A (AbdA) expression (Cenci and Gould, 2005). AbdA is a Hox protein expressed in the abdominal neuroblasts that activates the proapoptotic genes *rpr*, *grim* and *hid*, inducing apoptosis (Bello *et al*., 2003). This study, together with our results, suggests that Grh has a role in the control of cell proliferation and apoptosis and that this regulation depends on the tissue and developmental context.

After assessing these two important parameters in growth control in the wing imaginal disc, we looked at the adult wing phenotype. In the *grh* overexpressing wings the posterior compartment was significantly smaller than control wings. This result seems consistent with the reduced cell proliferation and increased apoptosis observed in the wing discs at larval stages. On the other hand, the *grh* knockdown adult wings also presented a smaller posterior compartment than the controls, which suggests that, even though cell proliferation seems to be increased in the wing discs, those cells must be eliminated during metamorphosis. This phenotype also points to the possibility that the increased number of proliferating cells in the *grh* knockdown condition might induce apoptosis, acting as a mechanism of controlling cell number, as mentioned above. In contrast, in the *grh* overexpression

condition, we observed increased apoptosis and reduced cell proliferation. In this case, it is possible that Grh has a more direct role in the regulation of apoptosis. Since there is more Grh protein than in a wild-type situation, it is possible that the excess Grh protein outcompetes other transcription factors in the regulation of genes involved in the apoptosis pathway. Harrison and colleagues (2010) have shown that Grh competes with the transcriptional activator Zelda (Zld) in *Drosophila* embryos (Harrison *et al*., 2010), so it would be interesting to assess if a similar gene expression regulation happens in the wing disc.

Another interesting observation is that the wing size was affected not only in the posterior compartment, where we manipulated *grh* expression, but also in the anterior compartment, giving rise to overall smaller wings.

When compared to controls, the anterior compartment area is increased in *grh* overexpressing wings and it is reduced after *grh* knockdown. This suggests that the anterior compartment adjusts its growth upon changes in the posterior compartment. In the future, we would like to understand why this response is different upon *grh* overexpression and knockdown, since the posterior compartment growth is reduced in both cases.

It is known that compartments can grow relatively independently of each other (Simpson, 1976), but when cell death or cell division rates are manipulated in one compartment, the other compartment adjusts its growth dynamics so that the final wing size is the same as in the wild type (Martín and Morata, 2006, Milán *et al.*, 1997). Remarkably, a study has shown that the induction of the pro-apoptotic gene *hid* for 48 h, resulting in the loss of 40% of the wing disc, allows nearly full recovery of the size and pattern of the wing (Herrera and Martín, 2013). In the case of Grh, however, we found that the final wing size was different from the controls. One possible explanation for this is that our experimental assay does not give enough time for the flies to fully recover, or that the effect of manipulating *grh* expression is so severe that the final wing size cannot be restored. The severe effects induced by *grh* expression manipulation in the adult wing can also result from the influence of Grh in different cellular processes, consistent with our observations that Grh also seems to regulate cell proliferation and E-cadherin and actin levels.

4.3. Regulation of actin cytoskeleton and E-cadherin by Grh

In addition to cellular processes directly involved in tissue growth control, we also assessed the influence of Grh in F-actin and E-cadherin. These proteins are important components of the cell cytoskeleton and adhesion complexes, respectively, and are thus critical for epithelial integrity and homeostasis (van Roy and Berx, 2008; Pollard and Cooper, 2009). Both actin and E-cadherin have been implicated in epithelial tissue growth and cancer. For example, F-actin regulates tissue growth in *Drosophila* and mammalian cells through the Hippo pathway (Matsui and Lai, 2013). Additionally, E-cadherin misregulation is commonly associated with epithelial cancers. E-cadherin downregulation is typically associated with EMT and contributes to tumor invasion and metastasis (Frixen *et al*., 1991; Perl *et al*., 1998).

We have found that 12 h of *grh* knockdown induce an increase in E-cadherin levels, whereas *grh* overexpression produces the opposite phenotype, suggesting that Grh acts as a repressor of E-cadherin expression. Grh has been previously implicated in the regulation of E-cadherin, not only in *Drosophila* but also in vertebrates. In *Drosophila*, Grh-binding sites were identified in the E-cadherin gene (called *shotgun*). In addition, it was shown that *grh* mutant neuroblasts show reduced levels of E-cadherin while ectopic *grh* expression is sufficient to increase E-cadherin levels (Almeida and Bray, 2005). In mice, a similar connection between Grhl-2 and E-cadherin has been shown, namely that Grhl2 interacts with the regulatory regions of the E-cadherin gene and influences the expression levels of this adhesion molecule (Werth *et al.*, 2010). Additionally, in human breast cancer cell lines, *grhl-2* downregulation is accompanied by a reduction in E-cadherin expression and the upregulation of EMT markers (Cieply *et al*., 2012). Interestingly all these studies show that the expression levels of *grh* and E-cadherin follow the same tendency, while we observed the opposite effect. Since *grh* can function as an activator or repressor of gene expression depending on the tissue and developmental context (Bray and Kafatos, 1991; Tuckfield *et al*., 2002), it is possible that the regulation of E-cadherin in the wing disc is different from other epithelial tissues. Future work should determine whether E-cadherin expression at the mRNA level is altered upon manipulation of *grh* in the wing disc. Besides the regulation of E-cadherin expression, our data suggest that Grh might also control its localization. In the *grh* knockdown condition we observed E-cadherin abnormally localized in the lateral membrane in wing disc epithelial cells. It is possible that the mislocalization of E-cadherin has an impact in cell polarity and adhesion as well as cell differentiation (van Roy and Berx, 2008; Stemmler, 2008). It would be interesting to confirm this hypothesis using known markers for these cellular processes.

Regarding actin levels, our results show that there is an increase in F-actin signal intensity upon *grh* knockdown, suggesting a role of Grh in the regulation of the actin cytoskeleton. Unfortunately we did not have the chance to repeat this experiment with shorter periods of *grh* RNAi expression, and those results are important to assess how the phenotype evolves over time. Future perspectives include a further analysis of the actin phenotype in order to understand what are the mechanisms by which Grh may regulate F-actin dynamics.

It is plausible that Grh influences F-actin through the regulation of actin-binding proteins (ABPs). A microarray analysis performed in mutant *grh* embryos revealed that the genes regulated by Grh include several factors involved in actin organization (Paré *et al*., 2012). Some were upregulated, such as Capulet, an ABP that inhibits actin filament polymerization (Baum *et al*., 2000), while others were downregulated, as is the case of Fhos, which is a formin-like protein that promotes F-actin polymerization (Anhezini *et al*., 2012). Since Grh function can vary from one tissue to another it would be interesting to assess how Grh regulates actin and ABPs in the wing disc.

When expressing *grh* RNAi for 72 h we observed that both E-cadherin and F-actin levels were increased, not only in the posterior compartment, but in the entire wing disc, suggesting that Grh might have a cell non-autonomous effect. Alternatively, as in this experiment the *grh* knockdown was

performed for a long period of time (72 h), these phenotypes could also be a consequence of other cellular processes regulated by Grh.

For example, apoptotic cells are removed from the live tissue by extrusion. Several studies suggest that apoptotic cells induce E-cadherin and actin changes in the surrounding cells to promote extrusion (Rosenblatt *et al*., 2001; Lubkov and Bar-sagi, 2014; Shen and Dahmann, 2005). Considering that both *grh* knockdown and overexpression induce apoptosis, it is possible that some of the actin and E-cadherin changes observed in the wing disc are the result of this event.

4.4. *grh* mutant clones

We showed that *grh* RNAi was enough to successfully and specifically regulate *grh* expression. Nevertheless, some phenotypic variability was observed, which is typical of the RNAi technique. Since *grh* mutants are embryonic lethal (Nüsslein-Volhard *et al*., 1984), the generation of *grh* mutant clones is a great alternative to confirm our results as it allows the phenotypic analysis of a population of *grh* mutant cells in a wild-type tissue. We generated *grh* mutant clones using the FLP/FRT technique (Golic and Lindquist, 1989) and validated that Grh is absent specifically in that cell population.

Although we did not have the chance to further analyse the phenotype of *grh* mutant clones, we believe that this technique will help us to answer some of the open questions that arise from this thesis. We would like to assess if Grh can induce non-cell autonomous changes in E-cadherin and F-actin expression, as well as understand the dynamics between cell proliferation and apoptosis.

4.5. Concluding remarks

In summary, our results suggest that Grh is important to control wing growth in *Drosophila*. Overexpressing *grh* leads to massive apoptosis and severe reduction in cell proliferation, impairing tissue growth and development. When Grh levels are reduced there is an increase in cell proliferation also accompanied by apoptosis. In addition to the regulation of growth control mechanisms such as apoptosis and proliferation Grh also seems to regulate actin and E-cadherin, key components of the cell cytoskeleton and cell adhesion complexes that can have a major impact in the cell and tissue properties.

Our results reinforce the evolutionary conservation and relevance of Grh in the control of epithelial growth and integrity. In the future, we hope to contribute to a greater knowledge of Grh function in epithelia and the mechanism underlying it.

5. REFERENCES

Adams, M.D., Celniker, S.E., Holt, R.A., Evans, C.A., Gocayne, J.D., Amanatides, P.G., Scherer, S.E., Li, P.W., Hoskins, R.A., Galle, R.F., George, R.A., Lewis, S.E., Richards, S., Ashburner, M., Henderson, S.N, Sutton, G.G., Wortman, J.R., Yandell, M.D., Zhang, Q., Chen, L.X., Brandon, R.C., Rogers, Y.H., Blazej, R.G., Champe, M., Pfeiffer, B.D., Wan, K.H., Doyle, C., Baxter, E.G., Helt, G., Nelson, C.R., Gabor, G.L., Abril, J.F., Agbayani, A., An, H.J., Andrews-Pfannkoch, C., Baldwin, D., Ballew, R.M., Basu, A., Baxendale, J., Bayraktaroglu, L., Beasley, E.M., Beeson, K.Y., Benos, P.V., Berman, B.P., Bhandari, D., Bolshakov, S., Borkova, D., Botchan, M.R., Bouck, J., Brokstein, P., Brottier, P., Burtis, K.C., Busam, D.A., Butler, H., Cadieu, E., Center, A., Chandra, I., Cherry, J.M., Cawley, S., Dahlke, C., Davenport, L.B., Davies, P., de Pablos, B., Delcher, A., Deng, Z., Mays, A.D., Dew, I., Dietz, S.M., Dodson, K., Doup, L.E., Downes, M., Dugan-Rocha, S., Dunkov, B.C., Dunn, P., Durbin, K.J., Evangelista, C.C., Ferraz, C., Ferriera, S., Fleischmann, W., Fosler, C., Gabrielian, A.E., Garg, N.S., Gelbart, W.M., Glasser, K., Glodek, A., Gong, F., Gorrell, J.H., Gu, Z., Guan, P., Harris, M., Harris, N.L., Harvey, D., Heiman, T.J., Hernandez, J.R., Houck, J., Hostin, D., Houston, K.A., Howland, T.J., Wei, M.H., Ibegwam, C., Jalali, M., Kalush, F., Karpen, G.H., Ke, Z., Kennison, J.A., Ketchum, K.A., Kimmel, B.E., Kodira, C.D., Kraft, C., Kravitz, S., Kulp, D., Lai, Z., Lasko, P., Lei, Y., Levitsky, A.A., Li, J., Li, Z., Liang, Y., Lin, X., Liu, X., Mattei, B., McIntosh, T.C., McLeod, M.P., McPherson, D., Merkulov, G., Milshina, N.V., Mobarry, C., Morris, J., Moshrefi, A., Mount, S.M., Moy, M., Murphy, B., Murphy, L., Muzny, D.M., Nelson, D.L., Nelson, D.R., Nelson, K.A., Nixon, K., Nusskern, D.R., Pacleb, J.M., Palazzolo, M., Pittman, G.S., Pan, S., Pollard, J., Puri, V., Reese, M.G., Reinert, K., Remington, K., Saunders, R.D., Scheeler, F., Shen, H., Shue, B.C., Sidén-Kiamos, I., Simpson, M., Skupski, M.P., Smith, T., Spier, E., Spradling, A.C., Stapleton, M., Strong, R., Sun, E., Svirskas, R., Tector, C., Turner, R., Venter, E., Wang, A.H., Wang, X., Wang, Z.Y., Wassarman, D.A., Weinstock, G.M., Weissenbach, J., Williams, S.M., Woodage, T., Worley, K.C., Wu, D., Yang, S., Yao, Q.A., Ye, J., Yeh, R.F., Zaveri, J.S., Zhan, M., Zhang, G., Zhao, Q., Zheng, L., Zheng, X.H., Zhong, F.N., Zhong, W., Zhou, X., Zhu, S., Zhu, X., Smith, H.O., Gibbs, R.A., Myers, E.W., Rubin, G.M. and Venter, J.C. 2000. The genome sequence of *Drosophila* melanogaster. Science. 287(5461): 2185–2195.

Almeida, M.S. and Bray, S.J. 2005. Regulation of post-embryonic neuroblasts by *Drosophila* Grainyhead. Mechanisms of Development. 122: 1282–1293.

Anhezini, L., Saita, A.P., Costa, M.S., Ramos, R.G. and Simon, C.R. 2012. Fhos encodes a *Drosophila* Formin-like protein participating in autophagic programmed cell death. Genesis. 50(9):672-84.

Ashburner, M., Golic, K.G. and Hawley, R.S. 2005. Life Cycle. *In Drosophila*. A Laboratory Handbook (John Inglis ed) 2nd ed., pp 121-205, Cold Spring Harbor Laboratoty Press, Cold Spring Harbor, New York

Auden, A., Caddy, J., Wilanowski, T., Ting, S.B., Cunningham, J.M., and Jane, S.M. 2006. Spatial and temporal expression of the Grainyhead-like transcription factor family during murine development. Genes Expression Patterns. 6:964–970.

Baum, B., Li, W. and Perrimon, N. 2000. A cyclase-associated protein regulates actin and cell polarity during *Drosophila* oogenesis and in yeast. Current Biology. 10:964–973.

Bello, B.C., Hirth, F. and Gould, A.P. 2003. A pulse of the *Drosophila* Hox protein Abdominal-A schedules the end of neural proliferation via neuroblast apoptosis. Neuron. 37:209-219.

Bhandari, A., Gordon, W., Dizon, D., Hopkin, A.S., Gordon, E., Yu, Z. and Andersen, B. 2013. The Grainyhead transcription factor Grhl3/Get1 suppresses miR-21 expression and tumorigenesis in skin: modulation of the miR-21 target MSH2 by RNA-binding protein DND1. Oncogene. 32:1497–1507.

Boglev, Y., Wilanowski, T., Caddy, J., Parekh, V., Auden, A., Darido, C., Hislop, N.R., Cangkrama, M., Ting, S.B., and Jane, S.M. 2011. The unique and cooperative roles of the Grainy head-like transcription factors in epidermal development reflect unexpected target gene specificity. Developmental Biology. 349:512–522.

Brand, A.H. and Perrimon, N. 1993. Targeted gene expression as a means of altering cell fates and generating dominant phenotypes. Development. 118: 401–415.

Bray, S.J., and Kafatos, F.C. 1991. Developmental function of Elf-1: An essential transcription factor during embryogenesis in *Drosophila*. Genes and Development. 5: 1672–1683.

Bryant, P.J. 1975. Pattern formation in the imaginal wing disc of *Drosophila* melanogaster: fate map, regeneration and duplication. The Journal of Experimental Zoology. 193: 49-78.

Bryant, P.J. and Simpson, P. 1984. Intrinsic and extrinsic control of growth in developing organs. The Quarterly Review of Biology. 59: 387-415.

Butler, M.J., Jacobsen, T.L., Cain, D.M., Jarman, M.G., Hubank, M., Whittle, J.R., Phillips, R. and Simcox, A. 2003. Discovery of genes with highly restricted expression patterns in the *Drosophila* wing disc using DNA oligonucleotide microarrays. Development. 130:659-670.

Caddy, J., Wilanowski, T., Darido, C., Dworkin, S., Ting, S.B., Zhao, Q., Rank, G., Auden, A., Srivastava, S., Papenfuss, T.A., Murdoch, J.N., Humbert, P.O., Parekh, V., Boulos, N., Weber, T., Zuo, J., Cunningham, J.M. and Jane, S.M. 2010. Epidermal wound repair is regulated by the planar cell polarity signaling pathway. Developmental Cell. 19:138–147.

Calleja, M., Moreno, E., Pelaz, S. and Morata, G. 1996. Visualization of gene expression in living adult *Drosophila*. Science. 274: 253–255.

Cenci, C., and Gould, A.P. 2005. *Drosophila* Grainyhead specifies late programmes of neural proliferation by regulating the mitotic activity and Hox-dependent apoptosis of neuroblasts. Development. 132:3835–3845.

Cieply, B., Farris, J., Denvir, J., Ford, H.L. and Frisch, S.M. 2013. Epithelial-Mesenchymal Transition and Tumor Suppression Are Controlled by a Reciprocal Feedback Loop between ZEB1 and Grainyhead-like-2. Cancer Research. 73(20):6299-6309.

Cieply, B., Riley, P.4th, Pifer, P.M., Widmeyer, J., Addison, J.B., Ivanov, A.V, Denvir, J., Frisch, S.M. 2012. Suppression of the epithelial-mesenchymal transition by Grainyhead-like-2. Cancer Research. 72:2440–2453.

Cohen, S.M. 1993. Imaginal disc development. *In Drosophila* Development. (A. Martinez-Arias and M. Bate eds), pp. 747-841. Cold Spring Harbor: Cold Spring Harbor Press, New York

Darido,C., Georgy, S.R., Wilanowski, T., Dworkin, S., Auden,A., Zhao,Q., Rank,G., Srivastava, S., Finlay, M.J., Papenfuss, A.T., Pandolfi, P.P, Pearson, R.B. and and Jane, S.M. 2011. Targeting of the tumor suppressor GRHL3 by a miR-21-dependent proto-oncogenic network results in PTEN loss and tumorigenesis. Cancer Cell. 20:635–648.

Dhanasekaran, D.N. and Reddy, E.P. 2008. JNK signaling in apoptosis. Oncogene. 27: 6245–6251.

Dietzl, G., Chen, D., Schnorrer, F., Su, K.C., Barinova, Y,. Fellner, M., Gasser, B., Kinsey, K., Oppel, S., Scheiblauer, S., Couto, A., Marra, V., Keleman, K. and Dickson, B.J. 2007. A genome-wide transgenic RNAi library for conditional gene inactivation in *Drosophila*. Nature. 448:151–156.

Edgar, B.A. 2006. How flies get their size: genetics meets physiology. Nature Reviews. Genetics. 7:907–916.

Elliott, D.A. and Brand, A.H. 2008. The Gal4 System. A Versatile System for the Expression of Genes. *In* Methods in Molecular Biology: *Drosophila*: Methods and Protocols (C. Dahmann ed), pp 79–95, Humana Press Inc., Totowa, NJ.

Fabian, J., Lodrini, M., Oehme, I., Schier, M.C., Thole, T.M., Hielscher, T., Kopp-Schneider, A., Opitz, L., Capper, D., von Deimling, A., Wiegand, I., Milde, T., Mahlknecht, U.,Westermann, F., Popanda, O., Roels, F., Hero, B., Berthold, F., Fischer, M., Kulozik, A.E., Witt, O. and Deubzer, H.E. 2014. GRHL1 acts as tumor suppressor in neuroblastoma and is negatively regulated by MYCN and HDAC3. Cancer Research. 74(9):2604-16.

Fan, Y. and Bergmann, A. 2008. Distinct mechanisms of apoptosis-induced compensatory proliferation in proliferating and differentiating tissues in the *Drosophila* eye.Dev. Cell. 14: 399–410.

Faulstich, H., Zobeley, S., Rinnerthaler, G. and Small, J.V. 1988. Fluorescent phallotoxins as probes for filamentous actin. Journal of Muscle Research and Cell Motility. 9(5):370-83.

Fire, A., Xu, S., Montgomery, M.K., Kostas, S.A., Driver, S.E. and Mello, C.C. 1998. Potent and specific genetic interference by double-stranded RNA in *Caenorhabditis elegans*. Nature. 391:806–811.

Frixen U. H., Behrens J., Sachs M., Eberle G., Voss B., Warda A., Lçchner D. and Birchmeier W. 1991. E-cadherin mediated cell-cell adhesion prevents invasiveness of human carcinoma cells. The Journal of Cell Biology. 113:173 – 185.

Garcia-Bellido, A. and Merriam, J. 1971. Parameters of the wing imaginal disc development of *Drosophila* melanogaster. Developmental Biology. 24: 61-87.

Golic, K.G., and Lindquist, S. 1989. The FLP recombinase of yeast catalyzes site-specific recombination in the *Drosophila* genome. Cell. 59: 499–509.

Gonzalez-Gaitan, M., Capdevila, M. P. and Garcia-Bellido, A. 1994. Cell proliferation patterns in the wing imaginal disc of *Drosophila*. Mechanisms of Development. 46:183–200.

Goyal, L., Mccall, K., Agapite, J., Hartwieg, E. and Steller, H. 2000. Induction of apoptosis by *Drosophila* reaper, hid and grim through inhibition of IAP function. EMBO Journal.19: 589–597.

Grewal, S.S. 2008. Insulin/TOR signaling in growth and homeostasis: A view from the fly world. The International Journal of Biochemistry & Cell Biology. 41(5):1006-1010.

Hamaratoglu, F., Willecke, M., Kango-Singh, M., Nolo, R., Hyun, E., Tao, C., Jafar-Nejad, H. and Halder, G. 2006. The tumour-suppressor genes NF2/Merlin and Expanded act through Hippo signalling to regulate cell proliferation and apoptosis. Nature Cell Biology. 8:27-36.

Hans, F. and Dimitrov, S. 2001. Histone H3 phosphorylation and cell division. Oncogene. 20(24):3021-3027.

Harrison, M.M., Botchan, M.R., and Cline, T.W. 2010. Grainyhead and Zelda compete for binding to the promoters of the earliest-expressed *Drosophila* genes. Developmental Biology. 345:248–255.

Hemphala, J., Uv, A., Cantera, R., Bray, S. and Samakovlis, C. 2003. Grainy head controls apical membrane growth and tube elongation in response to Branchless/FGF signalling. Development. 130: 249–258.

Hendzel, M.J., Wei, Y., Mancini, M.A., Van Hooser, A., Ranalli, T., Brinkley, B.R., Bazett-Jones, D.P. and Allis, C.D. 1997. Mitosis-specific phosphorylation of histone H3 initiates primarily within pericentromeric heterochromatin during G2 and spreads in an ordered fashion coincident with mitotic chromosome condensation. Chromosoma.106:348–360.

Hengartner, M.O. 2000. The biochemistry of apoptosis. Nature. 407:770–776.

Herrera, S.C., Martín, R. and Morata, G. 2013. Tissue Homeostasis in the Wing Disc of *Drosophila* melanogaster: Immediate Response to Massive Damage during Development. PLoS Genetics. 9(4):e1003446.

Igaki, T., Pagliarini, R.A. and Xu, T. 2006. Loss of cell polarity drives tumor growth and invasion through JNK activation in *Drosophila*. Current Biology. 16(11):1139-46.

Igaki, T., Pastor-Pareja, J.C., Aonuma, H., Miura, M., Xu, T. 2009. Intrinsic tumor suppression and epithelial maintenance by endocytic activation of Eiger/TNF signaling in *Drosophila*. Developmental Cell. 16(3):458-65.

James, A. A. and Bryant, P.J.1981. Mutations causing pattern deficiencies and duplications in the imaginal wing disk of *Drosophila* melanogaster. Developmental Biology. 85:39-54.

Kerr, J.F., Wyllie, A.H., and Currie, A.R. 1972. Apoptosis: a basic biological phenomenon with wide-ranging implications in tissue kinetics. British Journal of Cancer. 26:239–257.

Kim, M. and McGinnis, W. 2010. Phosphorylation of Grainy head by ERK is essential for wound-dependent regeneration but not for development of an epidermal barrier. Proceedings of the National Academy of the United Stated of America. 108(2):650-5.

Kondo, S., Senoo-Matsuda, N., Hiromi, Y. and Miura, M. 2006. DRONC coordinates cell death and compensatory proliferation. Molecular and Cellular Biology. 26:7258–7268.

Kumar, S. and Doumanis, J. 2000. The fly caspases, Cell Death & Differentiation. 7:1039–1044.

Lawrence, P. A. and Morata, G. 1977. The early development of mesothoracic compartments in *Drosophila*. An analysis of cell lineage and fate mapping and an assessment of methods. Developmental Biology. 56:40-51.

Lee, H., and Adler, P.N. 2004. The grainy head transcription factor is essential for the function of the frizzled pathway in the *Drosophila* wing. Mechanisms of Development.121:37–49.

Lee, T. and Luo, L. 1999. Mosaic analysis with a repressible cell marker for studies of gene function in neuronal morphogenesis. Neuron. 22: 451–61.

Llense, F. and Martín-Blanco E. 2008. JNK signaling controls border cell cluster integrity and collective cell migration. Current Biology. 18(7):538-44.

Lohmann, I., McGinnis, N., Bodmer, M. and McGinnis, W. 2002. The *Drosophila* Hox gene deformed sculpts head morphology via direct regulation of the apoptosis activator reaper. Cell. 2002. 110(4):457-66.

Lubkov, V., Bar-Sagi, D. 2014. E-cadherin -mediated cell coupling is required for apoptotic cell extrusion. Current Biology. 24(8):868-874.

Mace, K.A., Pearson, J.C., and McGinnis, W. 2005. An epidermal barrier wound repair pathway in *Drosophila* is mediated by grainy head. Science. 308: 381–385.

Madhavan, M.M. and Schneiderman, H.A. 1977. Histological analysis of the dynamics of growth of imaginal discs and histoblasts nests during the larval development of *Drosophila* melanogaster. Wilhelm Roux´s Archives. 183:269-305.

Manjón, C., Sánchez-Herrero, E. and Suzanne, M. 2007. Sharp boundaries of Dpp signalling trigger local cell death required for *Drosophila* leg morphogenesis. Nature Cell Biology. 9(1):57-63.

Martín, F.A. and Morata, G. 2006. Compartments and the control of growth in the *Drosophila* wing imaginal disc. Development. 133(22):4421-4426.

Martín-Blanco, E., Gampel, A., Ring, J., Virdee, K., Kirov, N., Tolkovsky, A.M. and Martinez-Arias. A. 1998. puckered encodes a phosphatase that mediates a feedback loop regulating JNK activity during dorsal closure in *Drosophila*. Genes & Development. 12(4):557-70.

Matsui, Y. and Lai, Z.C. 2013. Mutual regulation between Hippo signaling and actin cytoskeleton. Protein & Cell. 4:904–10.

Matsumoto, K., Toh-e, A., and Oshima,Y. 1978. Genetic control of galactokinase synthesis in Saccharomyces cerevisiae: evidence for constitutive expression of the positive regulatory gene Gal4. Journal of Bacteriology. 134(2): 446-57.

McEwen, D.G. and Peifer, M. 2005. Puckered, a *Drosophila* MAPK phosphatase, ensures cell viability by antagonizing JNKinduced apoptosis. Development. 132: 3935–3946.

McGuire, S.E., Le, P.T., Osborn, A.J., Matsumoto, K. and Davis, R.L. 2003. Spatiotemporal rescue of memory dysfunction in *Drosophila*. Science. 302: 1765–1768.

Meister, G. and Tuschl, T. 2004. Mechanisms of gene silencing by double-stranded RNA. Nature. 431: 343–349.

Menéndez, J., Pérez-Garijo, A., Calleja, M. and Morata, G. 2010. A tumor-suppressing mechanism in *Drosophila* involving cell competition and the Hippo pathway. Proceedings of the National Academy of the United Stated of America. 107(33):14651-6.

Milán, M., Campuzano, S. and Garcia-Bellido, A. 1996. Cell cycling and patterned cell proliferation in the wing primordium of *Drosophila*. Proceedings of the National Academy of the United Stated of America. 93(2):640-645.

Milán, M., Campuzano, S. and Garcia-Bellido, A. 1997. Developmental parameters of cell death in the wing disc of *Drosophila*. Proceedings of the National Academy of the United Stated of America. 94(11):5691-6.

Morata, G., Shlevkov, E. and Pérez-Garijo, A. 2011. Mitogenic signaling from apoptotic cells in *Drosophila*. Development, Growth & Differentiation. 53(2):168-76.

Narasimha, M., Uv, A., Krejci, A., Brown, N.H., and Bray, S.J. 2008. Grainy head promotes expression of septate junction proteins and influences epithelial morphogenesis. Journal of Cell Science. 121:747–752.

Neto-Silva R.M., Wells B.S., Johnston L.A. 2009. Mechanisms of growth and homeostasis in the *Drosophila* wing. Annual Review of Cell and Developmental Biology. 25: 197-220.

Nicholson, D.W., Ali, A., Thornberry, N.A., Vaillancourt, J.P, Ding, C.K., Gallant, M., Gareau, Y., Griffin, P.R., Labelle, M., Lazebnik, Y.A, Munday, N.A, Raju, S.M., Smulson, M.E., Yamin, T., Yu, V.L. and Miller, D.K. 1995. Identification and inhibition of the ICE/CED-3 protease necessary for mammalian apoptosis. Nature. 376(6535):37-43.

Nüsslein-Volhard, C., Wieschaus, E. and Kluding, H. 1984. Mutations affecting the pattern of the larval cuticle in *Drosophila* melanogaster I. Zygotic loci on the second chromosome. Wilhelm Roux's Archives of Developmental Biology. 193:267-282.

Pan, D. 2007. Hippo signaling in organ size control. Genes & Development. 21:886–97.

Panis, C., Pizzatti, L., Herrera, A.C., Cecchini, R. and Abdelhay, E. 2013. Putative circulating markers of the early and advanced stages of breast cancer identified by high-resolution label-free proteomics. Cancer Letters. 330:57–66.

Paré, A., Kim, M., Juarez, M. T., Brody, S. and McGinnis, W. 2012. The functions of grainy head-like proteins in animals and fungi and the evolution of apical extracellular barriers. PLoS One. 7:e36254.

Pastor-Pareja, J.C. and Xu, T. 2013. Dissecting Social Cell Biology and Tumors Using *Drosophila* Genetics. Annual Review of Genetics. 47:69–92.

Pastor-Pareja, J.C., Grawe, F., Martín-Blanco, E., Garcia-Bellido, A., 2004. Invasive cell behaviour during *Drosophila* imaginal disc eversion is mediated by the JNK signalling cascade. Developmental Cell. 7:387-399.

Pearson, J.C., Juarez, M.T., Kim, M., Drivenes, O. and McGinnis, W. 2009. Multiple transcription factor codes activate epidermal wound-response genes in *Drosophila*. Proceedings of the National Academy of the United Stated of America. 106:2224–2229.

Perl A.K., Wilgenbus P., Dahl U., Semb H. and Christofori G. 1998. A causal role for E-cadherin in the transition from adenoma to carcinoma. Nature 392,:190 – 193.

Perrimon, N. 1998. Creating mosaics in *Drosophila*. The International journal of developmental biology. 42: 243–7.

Peters, L.M., Anderson, D.W., Griffith, A.J., Grundfast, K.M., San Agustin, T.B., Madeo, A.C., Friedman, T.B. and Morell, R.J. 2002. Mutation of a transcription factor, TFCP2L3, causes progressive autosomal dominant hearing loss, DFNA28. Human Molecular Genetics.11:2877–2885.

Petrof, G., Nanda, A., Howden, J., Takeichi, T., McMillan, J.R., Aristodemou, S., Ozoemena, L., Liu, L., South, A.P., Pourreyron, C., Dafou, D., Proudfoot, L.E., Al-Ajmi, H., Akiyama, M., McLean, W.H., Simpson, M.A., Parsons, M. and McGrath, J.A. 2014. Mutations in GRHL2 Result in an Autosomal-Recessive Ectodermal Dysplasia Syndrome. American Journal of Human Genetics.

95(3):308-14.

Pollard, T.D. and Cooper, J.A. 2009. Actin, a central player in cell shape and movement. Science. 326(5957):1208-1212.

Purves, D.C. and Brachmann, C. 2007. Dissection of Imaginal Discs from 3rd Instar *Drosophila* Larvae. Journal of Visualized Experiments. 2:e140.

Reiter, L.T., Potocki, L., Chien, S., Gribskov, M. and Bier, E. 2001. A systematic analysis of human disease-associated gene sequences in *Drosophila* melanogaster. Genome Research. 11(6):1114-25.

Ring, J.M. and Martinez Arias, A. 1993. puckered, a gene involved in position-specific cell differentiation in the dorsal epidermis of the *Drosophila* larva. Development. Supplement. 251-259.

Rosenblatt, J., Raff, M.C. and Cramer, L.P. 2001. An epithelial cell destined for apoptosis signals its neighbors to extrude it by an actin- and myosin-dependent mechanism. Current Biology. 11:1847–1857.

Ryoo, H.D., Gorenc, T. and Steller, H. 2004. Apoptotic cells can induce compensatory cell proliferation through the JNK and the wingless signaling pathways. Developmental Cell. 7:491-501.

Scholnick, S.B., Morganand, B.A. and Hirsh, J. 1983. The cloned Dopa decarboxylase gene is developmentally regulated when reintegrated into the *Drosophila* genome. Cell. 34:37–45.

Shen, J. and Dahmann, C. 2005. Extrusion of cells with inappropriate Dpp signaling from *Drosophila* wing disc epithelia. Science. 307(5716):1789-1790.

Simpson P. 1976. Analysis of the compartments of the wing of *Drosophila* melanogaster mosaic for a temperature-sensitive mutation that reduces mitotic rate. Developmental Biology. 54(1):100-15.

St. Pierre, S.E., Ponting, L., Stefancsik, R., McQuilton, P. and the FlyBase Consortium. 2014. FlyBase 102 - advanced approaches to interrogating FlyBase. Nucleic Acids Research. 42(D1):D780-D788. http://flybase.org/

Staley, B.K. and Irvine, K.D. 2012. Hippo signaling in *Drosophila*: recent advances and insights. Developmental Dynamics. 241:3–15.

Staveley, B.E. 2014. Molecular & Developmental Biology (BIOL3530). Organogenesis. Version 9 September 2014. http://www.mun.ca/biology/desmid/brian/BIOL3530/DB_09/DBNOrgan.html. in Memorial University of Newfoundland, Department of Biology, http://www.mun.ca/biology/.

Stemmler, M. P. 2008. Cadherins in development and cancer. Molecular BioSystems 4(8):835–850, 2008.

Suster, M.L., Seugnet, L., Bate, M. and Sokolowski, M. B. 2004. Refining Gal4-driven transgene expression in *Drosophila* with a Gal80 enhancer-trap. Genesis. 39: 240–5.

Tabata, T. and Takei, Y. 2004. Morphogens, their identification and regulation. Development. 131: 703–712.

Tanaka, Y., Kanai, F., Tada, M., Tateishi, R., Sanada, M., Nannya, Y., Ohta, M., Asaoka, Y., Seto, M., Shiina, S., Yoshida, H., Kawabe, T., Yokosuka, O., Ogawa, S. and Omata, M. 2008. Gain of GRHL2 is associated with early recurrence of hepatocellular carcinoma. Journal of Hepatololgy. 49:746–757.

Ting, S.B., Caddy, J., Hislop, N., Wilanowski, T., Auden, A., Zhao, L.L., Ellis, S., Kaur, P., Uchida,

Y., Holleran, W.M., Elias, P.M., Cunningham, J.M. and Jane, S.M. 2005. A homolog of *Drosophila* grainy head is essential for epidermal integrity in mice. Science. 308:411–413.

Tuckfield, A., Clouston, D.R., Wilanowski, T.M., Zhao, L.L., Cunningham, J.M., and Jane, S.M. 2002. Binding of the RING polycomb proteins to specific target genes in complex with the grainyhead-like family of developmental transcription factors. Molecular Cell Biology. 22:1936–1946.

Uv, A.E., Harrison, E.J., and Bray, S.J. 1997. Tissue-specific splicing and functions of the *Drosophila* transcription factor Grainyhead. Molecular Cell Biology. 17: 6727–6735.

Van Laer, L., Van Eyken, E., Fransen, E., Huyghe, J.R., Topsakal, V., Hendrickx, J.J., Hannula, S., Maki-Torkko, E., Jensen, M., Demeester, K., Baur, M., Bonaconsa, A., Mazzoli. M., Espeso, A., Verbruggen, K., Huyghe, J., Huygen, P., Kunst, S., Manninen, M., Konings, A., Diaz-Lacava, A.N., Steffens, M., Wienker, T.F., Pyykkö, I., Cremers, C.W., Kremer, H., Dhooge, I., Stephens, D., Orzan, E., Pfister, M., Bille, M., Parving, A., Sorri, M., Van de Heyning, P.H. and Van Camp, G. 2008. The grainyhead like 2 gene (GRHL2), alias TFCP2L3, is associated with age-related hearing impairment. Human Molecular Genetics.17:159–169.

Van Roy, F. and Berx, G. 2008. The cell-cell adhesion molecule E-cadherin . Cellular and Molecular Life Sciences. 65(23):3756-3788.

Wang, S. and Samakovlis, C. 2012. Grainy head and its target genes in epithelial morphogenesis and wound healing. Current Topics in Developmental Biology. 98: 35–63.

Wang, S., Tsarouhas, V., Xylourgidis, N., Sabri, N., Tiklova, K., Nautiyal, N., Gallio, M. and Samakovlis, C. 2009. The tyrosine kinase Stitcher activates Grainy head and epidermal wound healing in *Drosophila*. Nature Cell Biology.11:890–895.

Weigmann, K., Klapper, R., Strasser, T., Rickert, C., Technau, G., Jäckle, H., Janning, W. and Klämbt, C. 2003. FlyMove – a new way to look at development of *Drosophila*. Trends in Genetics:TIG. 19(6):310-1. http://flymove.uni-muenster.de

Werner, S., Frey, S., Riethdorf, S., Schulze, C., Alawi, M., Kling, L., Vafaizadeh, V., Sauter, G., Terracciano, L., Schumacher, U., Pantel, K. and Assmann, V. 2013. Dual roles of the transcription factor grainyhead-like 2 (GRHL2) in breast cancer. Journal of Biological Chemistry. 288(32):22993-3008.

Werth M., Walentin K., Aue A., Schönheit J., Wuebken A., Pode-Shakked N., Vilianovitch L., Erdmann B., Dekel B., Bader M., Barasch J., Rosenbauer F., Luft F.C. and Schmidt-Ott K.M. 2010. The transcription factor grainyhead-like 2 regulates the molecular composition of the epithelial apical junctional complex. Development. 137:3835–3845.

Wilson, R., Goyal, L., Ditzel, M., Zachariou, A., Baker, D.A., Agapite, J., Steller, H. and Meier, P. 2002. The DIAP1 RING finger mediates ubiquitination of Dronc and is indispensable for regulating apoptosis. Nature Cell Biology. 4:445–450.

Xiang, J., Fu, X., Ran, W., Chen, X., Hang, Z., Mao, H. and Wang Z. 2013. Expression and role of grainyhead-like 2 in gastric cancer. Medical Oncology. 30(4):714.

Xiang, X., Deng, Z., Zhuang, X., Ju, S., Mu, J., Jiang, H., Zhang, L., Yan, J., Miller, D. and Zhang, H.G. 2012. Grhl2 determines the epithelial phenotype of breast cancers and promotes tumor progression. PLoS One. 7(12):e50781.

Xu, H., Liu, C., Zhao, Z., Gao, N., Chen, G., Wang, Y. and Cui, J. 2014. Clinical implications of GRHL3 protein expression in breast cancer. Tumour Biology. 35(3):1827-31.

Yamamoto-Hino, M. and Goto, S. 2013. In Vivo RNAi-Based Screens: Studies in Model Organisms. Genes. 4:646–665.

Yu, Z., Lin, K.K., Bhandari, A., Spencer, J.A., Xu, X., Wang, N., Lu, Z., Gill, G.N., Roop, D.R., Wertz, P., and Andersen, B. 2006. The Grainyhead-like epithelial transactivator Get-1/Grhl3 regulates epidermal terminal differentiation and interacts functionally with LMO4. Developmental Biology. 299:122–136.

Zhao, B., Li, L,, Lei, Q,, Guan, K,L. 2010. The Hippo-YAP pathway in organ size control and tumorigenesis: an updated version. Genes & Development. 24(9):862-74.